TRAILING EDGE NOISE
EVALUATED AT VERY LOW MACH NUMBER
FROM INCOMPRESSIBLE FLOW SIMULATIONS

M. S. Howe
Boston University, College of Engineering
110 Cummington Street, Boston MA 02215
8 March, 1999

Report AM-99-003

BOSTON UNIVERSITY

Department of Aerospace and Mechanical Engineering

110 Cummington Street
Boston, Massachusetts 02215

TRAILING EDGE NOISE
EVALUATED AT VERY LOW MACH NUMBER
FROM INCOMPRESSIBLE FLOW SIMULATIONS

M. S. Howe
Boston University, College of Engineering
110 Cummington Street, Boston MA 02215
8 March, 1999

Report AM-99-003

Final Report
Prepared for Dr. L. Patrick Purtell
Office of Naval Research, Code 333
Grant N00014-98-1-0798

CONTENTS

CHAPTER 1

TRAILING EDGE NOISE AT LOW MACH NUMBERS

SUMMARY

A review is made of the diffraction theory of the trailing edge noise generated by a flat-plate airfoil of zero-thickness and non-compact chord, according to which the sound is attributed to the scattering of a 'frozen' pattern of turbulence wall pressure swept over the edge in the mean flow. Extension is made to determine the sound produced by very low Mach number flow over the edge of an airfoil of finite thickness. In applications it is desirable to represent the noise in terms of a surface integral over the airfoil involving a Green's function and a metric of the edge flow that can be calculated locally using the equations of motion of an *incompressible* fluid. It is argued that the appropriate metric for a rigid airfoil is the incompressible 'upwash' velocity (determined by the Biot-Savart induction formula applied to the boundary layer vorticity outside the viscous sublayer), and *not* the surface pressure. Formulae for calculating the noise are given when the airfoil thickness is acoustically compact, and for both three and two-dimensional edge flows.

The theory is illustrated by a detailed discussion of a two-dimensional vortex flow over an airfoil with a rounded trailing edge. The problem is simple enough to be treated analytically, yet is also suitable for validating computational edge noise schemes.

1. INTRODUCTION

The 'self-noise' generated by an airfoil in a nominally steady, high Reynolds number flow is attributed to the instability of the airfoil boundary layers and their interactions with the trailing edge [1 - 3]. The edge is usually a source of high frequency sound associated with smaller scale components of the boundary layer turbulence. Low frequency contributions from a trailing edge, that may in practice be related to large scale vortical structures shed from an upstream appendage, are small because the upwash velocity they produce in the neighborhood of the edge tends to be cancelled by that produced by vorticity shed from the edge [4, 5]. If the surface S of the airfoil is *rigid*, and is at rest in a mean stream, the far field acoustic pressure $p'(\mathbf{x},t) \equiv p(\mathbf{x},t) - p_o$ at position $\mathbf{x}$ and time t ($p(\mathbf{x},t)$ being the pressure and p_o its mean value in the acoustic far field) is given formally by Curle's [6, 7] formula

$$p'(\mathbf{x},t) = \frac{\partial^2}{\partial x_i \partial x_j} \int_V \left[T_{ij}\right] \frac{d^3\mathbf{y}}{4\pi|\mathbf{x}-\mathbf{y}|} - \frac{\partial}{\partial x_i} \oint_S \left[p'_{ij}\right] \frac{dS_j(\mathbf{y})}{4\pi|\mathbf{x}-\mathbf{y}|}, \quad |\mathbf{x}| \to \infty, \tag{1}$$

where the first integral is over the volume V occupied by the fluid, the surface element dS_j is directed into V,

$$p'_{ij} = (p - p_o)\delta_{ij} - \sigma_{ij}, \tag{2}$$

and σ_{ij} is the viscous stress tensor. The square brackets [ ] in (1) denote evaluation of the contents at the retarded time $t - |\mathbf{x}-\mathbf{y}|/c_o$, where c_o is the speed of sound. The direct sound generated by the turbulence *quadrupoles* [8, 9] is represented by the first integral in (1). At low Mach numbers (e.g. underwater) $T_{ij} \approx \rho_o v_i v_j$ per unit volume (ρ_o and $\mathbf{v}$ being respectively the mean fluid density and the velocity), and the quadrupole noise is usually negligible compared with that from the edge. The latter is contained in the surface integral in (1), and for an *acoustically compact* surface (for example, an airfoil whose chord is much smaller than the typical acoustic wavelength), the edge noise is equivalent to that generated by a distribution of *dipoles* on S, whose strength per unit area is the unsteady surface pressure [8, 9]. In that case the ratio of the acoustic powers generated by the edge and the volume quadrupoles $\sim$ $O(1/M^2)$, where $M \sim v/c_o \ll 1$ is the characteristic Mach number [6]. At high frequencies, when it is not permissible to assume the chord to be compact, the relative efficiency of the edge noise is increased to $O(1/M^3)$ [10].

For the compact chord airfoil the dipole strengths can be determined to a sufficient approximation for use in (1) by a preliminary calculation of the flow near the edge in which the influence of compressibility is ignored. However, although (1) is exact for a non-compact

airfoil, it is not permissible to neglect compressibility when specifying the dipole strengths in the surface integral. Therefore, edge noise predictions have traditionally been made by one of two alternative procedures. In the first, it is assumed that the trailing edge is well approximated by a semi-infinite, rigid plate. A calculation is then performed in which the free field *hydrodynamic* pressure p_I, say, generated by the boundary layer turbulence is *diffracted* by the edge. If p_I were known exactly this procedure would yield an accurate prediction of the edge generated sound. Hitherto it has not been possible to prescribe with sufficient accuracy the influence of the edge on the hydrodynamic pressure, and it has usually been assumed that the turbulence is swept past the edge by the mean flow as a *frozen* distribution of vorticity [1, 11 - 15]. In the second method, the noise is calculated by the acoustic analogy theory of Lighthill [8, 9] using a *compact* Green's function tailored to the trailing edge geometry [16, 17] (as opposed to the free space Green's function used in Curle's equation (1)). The sound can then be expressed directly in terms of the vorticity in the edge flow (calculated as if the flow is incompressible); this approach also enables the frozen approximation of the first method to be extended to more complicated trailing edge geometries [17].

Modern computational procedures will soon yield accurate predictions of the high Reynolds number hydrodynamic motion near a trailing edge, and it is appropriate to re-evaluate the kind of numerical data that will be required to make confident predictions of the far field sound. We have suggested above that an incompressible approximation to the surface pressure is *not* sufficient when the surface is not compact. This is because a non-compact body extends into the acoustic far field, and any representation of the sound as a Curle (or Kirchhoff) type of surface integral must ensure that the boundary conditions on the surface continue to be satisfied in the far field. This can be done either by using a Green's function tailored to the airfoil characteristics or (as in (1)) by using the free space Green's function, but with p'_{ij} known to the required precision *in the acoustic domain.* In the latter case the dipole strength must be prescribed with full account taken of compressibility, which is not normally possible because it presupposes a knowledge of the acoustic field at the surface [18]. In fact, the dipole strength can safely be estimated from an incompressible edge flow model only when the airfoil is acoustically compact. In general, the surface source strength turns out to depend on the *upwash* produced by the unsteady flow. When this is known (in an incompressible approximation) the edge noise can be found by using an acoustic Green's function whose normal derivative vanishes on the rigid surface

of the airfoil.

In this chapter the thin-plate diffraction theory of trailing edge noise is first reviewed (§2), and predictions are used to exhibit explicitly the failure of approximations based on (1). The general edge noise problem at low Mach numbers is then formulated in terms of the theory of vortex sound, and it is demonstrated how the the sound can be determined from an incompressible approximation to the 'upwash' velocity (§3). The theory is illustrated by a detailed application (§4) to determine the noise produced in a low Mach number vortex flow past the rounded trailing edge of a thick airfoil.

2. THIN-PLATE MODEL OF TRAILING EDGE NOISE

2.1 Diffraction theory [11, 12]

Consider turbulent trailing edge flow over the *upper* surface $x_2 = +0$ of the rigid half-plane $x_1 < 0$, $x_2 = 0$, where the main stream outside the boundary layers has low subsonic speed U in the x_1-direction (Figure 1). The calculation of the edge noise is formulated as a scattering or diffraction problem, in which the pressure $p_{\rm I}$, say, that would be produced by the same turbulent flow if the surface were absent, is scattered by the edge. The scattered pressure p' includes both acoustic and hydrodynamic components, the latter accounting for the modification of the near field pressure by the surface. The condition that the normal velocity vanishes on the half-plane is taken in the high Reynolds number approximation

$$\partial p_{\rm I}/\partial x_2 + \partial p'/\partial x_2 = 0, \quad \text{on S}, \tag{3}$$

where S denotes the 'upper' and 'lower' surfaces ($x_1 < 0$, $x_2 = \pm 0$). In turbulence-free regions, and when the mean stream Mach number $M = U/c_{\rm o}$ is very small, pressure fluctuations $p(\mathbf{x}, \omega)$ of frequency ω (with suppressed time factor $\mathrm{e}^{-i\omega t}$) satisfy the Helmholtz equation

$$(\nabla^2 + \kappa_{\rm o}^2)p = 0, \tag{4}$$

where $\kappa_{\rm o} = \omega/c_{\rm o}$ is the acoustic wavenumber. The presence of the boundary layer and the turbulence are ignored except insofar as they are responsible for the pressure $p_{\rm I}$; in particular $p'(\mathbf{x}, \omega)$ is assumed to satisfy (3) everywhere, and the scattering of sound by the shear flow is neglected. This approximation is not valid at very high frequencies when the acoustic wavelength is comparable to the thickness of the boundary layer.

The pressure $p_{\rm I}(\mathbf{x}, \omega)$ must be an outgoing solution of Helmholtz's equation in $x_2 \leq 0$, in the region 'below' the boundary layer sources; on $x_2 = 0$, $p_{\rm I}$ is equal to *half* the boundary layer *blocked pressure* p_s that the same turbulence would exert on an infinite plane wall at $x_2 = +0$, and we can write

$$p_{\rm I}(\mathbf{x}, \omega) = \frac{1}{2}\int_{-\infty}^{\infty} p_s(\mathbf{k}, \omega)\mathrm{e}^{i(\mathbf{k}.\mathbf{x} - \gamma(k_1)x_2)}dk_1 dk_3, \quad x_2 \leq 0, \quad \mathbf{k} = (k_1, 0, k_3), \tag{5}$$

where $\gamma(k) = \sqrt{\kappa_o^2 - k^2}$ is either real with sign $\mathrm{sgn}(\omega)$ or positive imaginary. The problem of calculating p' now reduces to the determination of the scattered pressure (from (3) and (4)) produced by the interaction of each Fourier component $\frac{1}{2}p_s(\mathbf{k}, \omega)\mathrm{e}^{i(\mathbf{k}.\mathbf{x} - \gamma(k)x_2)}$ of $p_{\rm I}$ with S.

The calculation can be performed by the Wiener-Hopf procedure [19], which supplies the following representation of the total perturbation pressure (which is finite at the edge of the half-plane)

$$p(\mathbf{x},\omega) = \frac{1}{2}\int_{-\infty}^{\infty} p_s(\mathbf{k},\omega)\mathrm{e}^{i(\mathbf{k}.\mathbf{x}+\gamma(k)|x_2|)}dk_1dk_3$$

$$- \frac{\mathrm{sgn}(x_2)}{4\pi i}\int_{-\infty}^{\infty} \frac{p_s(\mathbf{k},\omega)\sqrt{(\kappa_o^2-k_3^2)^{1/2}+k_1}}{\sqrt{(\kappa_o^2-k_3^2)^{1/2}+K_1}(K_1-k_1+i0)}\mathrm{e}^{i\{K_1x_1+k_3x_3+\gamma(K)|x_2|\}}dK_1dk_1dk_3, \qquad (6)$$

where $K=\sqrt{K_1^2+k_3^2}$. The first integral represents the direct pressure p_{I} (generated by the boundary layer 'in the absence of S'), and is strictly valid only outside the boundary layer in $x_2 \le 0$ or $x_2 > \delta$, where δ is the boundary layer thickness.

The integration with respect to K_1 can be performed explicitly when $x_2 \to \pm 0$. It is zero in the wake ($x_1 \ge 0$), where the scattered pressure vanishes. For $x_1 < 0$ the integration contour is displaced to $-i\infty$ in the K_1-plane, capturing the residue contribution from the pole at $K_1 = k_1 - i0$ and an integral along the branch cut of $\sqrt{(\kappa_o^2-k_3^2)^{1/2}+K_1}$, which extends from $-(\kappa_o^2-k_3^2)^{1/2}$, just below the real axis, to $-i\infty$. The branch-cut integral can be expressed in terms of the error function $\mathrm{erf}(x) = (2/\sqrt{\pi})\int_0^x \mathrm{e}^{-\lambda^2}d\lambda$ [20]. The total surface pressure is then found to be

$$p(x_1,\pm 0,x_3,\omega) = \frac{1}{2}\iint_{-\infty}^{\infty} p_s(\mathbf{k},\omega)\left[1 \pm \mathrm{erf}\left(\mathrm{e}^{-\frac{i\pi}{4}}|x_1|^{\frac{1}{2}}\sqrt{(\kappa_o^2-k_3^2)^{1/2}+k_1}\right)\right]\mathrm{e}^{i\mathbf{k}.\mathbf{x}}\,d^2\mathbf{k}, \quad x_1<0. \qquad (7)$$

The argument of the error function has positive real part for all real values of k_1, so that the error function ≈ 1 as $x_1 \to -\infty$. Thus, $p \to 0$ on the lower surface ($x_2 = -0$) far upstream of the edge, whereas $p \to p_s$ on the surface $x_2 = +0$ exposed to the turbulent stream. This occurs at distances upstream of the edge exceeding the characteristic eddy dimension. If the impinging boundary layer turbulence is assumed to be frozen during convection over the edge, measurements of the blocked pressure p_s several boundary layer thicknesses upstream of the edge can be used in the second integral of (6) to predict the edge noise.

At large distances from the edge the integrations with respect to K_1 and k_3 in the second integral of (6) may be performed by the method of stationary phase [19, 21]. This yields the edge-scattered acoustic pressure in the Chase-Chandiramani [11, 12] form

$$p'(\mathbf{x},\omega) \approx \frac{\kappa_o^{\frac{1}{2}}\sin^{\frac{1}{2}}\psi\sin(\theta/2)\mathrm{e}^{i\kappa_o|\mathbf{x}|}}{\sqrt{2}|\mathbf{x}|}\int_{-\infty}^{\infty}\frac{\sqrt{\kappa_o\sin\psi+k_1}}{(\kappa_o x_1/|\mathbf{x}|-k_1)}\,p_s(k_1,\kappa_o\cos\psi,\omega)dk_1, \quad |\mathbf{x}|\to\infty, \qquad (8)$$

where the angles θ, ψ defining the radiation direction $\mathbf{x}/|\mathbf{x}|$ are indicated in Figure 1.

The integrand in this formula is singular at $k_1 = \kappa_o x_1/|\mathbf{x}|$, where the stationary phase approximation breaks down. However, this occurs when k_1 lies in the *acoustic domain*, i.e., for a blocked pressure Fourier component $p_s(k_1, \kappa_o \cos\psi, \omega)$ that actually represents a sound wave generated by the boundary layer quadrupoles in the absence of the edge. Such contributions can be neglected at small Mach numbers. When the blocked surface pressure is regarded as entirely *hydrodynamic*, the remaining integral in (8) is dominated by wavenumbers $k_1 \sim \omega/U \gg \kappa_0$, and (8) reduces to

$$p'(\mathbf{x},\omega) \approx \frac{-\kappa_o^{\frac{1}{2}} \sin^{\frac{1}{2}}\psi \sin(\theta/2) e^{i\kappa_0|\mathbf{x}|}}{\sqrt{2}|\mathbf{x}|} \int_{-\infty}^{\infty} \frac{p_s(k_1,0,\omega)dk_1}{\sqrt{k_1+i0}}, \quad |\mathbf{x}| \to \infty. \tag{9}$$

This representation is suitable for expressing of the edge noise in terms of the hydrodynamic (i.e., *incompressible*) component of the blocked pressure measured upstream of the edge.

This is usually done by referring $p_s(k_1, 0, \omega)$ to the blocked surface pressure wavenumber-frequency spectrum $\mathrm{P}(\mathbf{k}, \omega)$ [22]. It is assumed that a finite section $-\frac{1}{2}L < x_3 < \frac{1}{2}L$, say, of the trailing edge is wetted by the turbulent flow, where L is much larger than the boundary layer thickness δ. Then, for statistically stationary turbulence

$$\langle p_s(k_1,0,\omega) p_s^*(k_1',0,\omega')\rangle \approx \frac{L}{2\pi}\delta(\omega-\omega')\delta(k_1-k_1')\mathrm{P}(k_1,0,\omega), \quad L \gg \delta, \tag{10}$$

where the angle brackets $\langle\ \rangle$ represent an ensemble average, and the asterisk denotes complex conjugate. The acoustic pressure frequency spectrum $\Phi(\mathbf{x},\omega)$ of the edge noise (defined such that $\langle p'^2(\mathbf{x},t)\rangle = \int_0^\infty \Phi(\mathbf{x},\omega)d\omega$) is then calculated from (9) to be given by

$$\Phi(\mathbf{x},\omega) \approx \frac{\omega L \sin^2(\theta/2)\sin\psi}{2\pi c_0|\mathbf{x}|^2} \int_{-\infty}^{\infty} \frac{\mathrm{P}(k_1,0,\omega)\, dk_1}{|k_1|}, \quad M \ll 1, \ \ |\mathbf{x}| \to \infty. \tag{11}$$

The peak acoustic pressures are radiated in the 'forward' directions $\theta = \pm\pi$. Numerical predictions are made by introducing a convenient empirical model for $\mathrm{P}(\mathbf{k},\omega)$ (see, e.g. [22, 23]), although this will not be discussed here.

2.2 Application of Curle's equation

To derive these results from Curle's representation (1), the first, quadrupole, integral on the right is discarded, and p'_{ij} is approximated by $(p-p_o)\delta_{ij}$ at high Reynolds numbers. Then for each component of the sound of frequency ω

$$p'(\mathbf{x},\omega) \approx -\frac{\partial}{\partial x_2}\int_{-\infty}^{\infty} dy_3 \int_{-\infty}^{0} [p(y_1,y_3)] \frac{e^{i\kappa_0|\mathbf{x}-\mathbf{y}|}}{4\pi|\mathbf{x}-\mathbf{y}|}\, dy_1, \quad \mathbf{y} = (y_1,0,y_3) \tag{12}$$

where

$$[p(x_1, x_3)] = p(x_1, +0, x_3, \omega) - p(x_1, -0, x_3, \omega) \tag{13}$$

is the pressure jump across the half-plane.

At large distances from the wetted edge

$$\frac{\partial}{\partial x_2}\left(\frac{\mathrm{e}^{i\kappa_0|\mathbf{x}-\mathbf{y}|}}{4\pi|\mathbf{x}-\mathbf{y}|}\right) \approx \frac{i\kappa_0 x_2 \mathrm{e}^{i\kappa_0|\mathbf{x}|}}{4\pi|\mathbf{x}|^2}\,\mathrm{e}^{-i\kappa_0\mathbf{x}\cdot\mathbf{y}/|\mathbf{x}|},$$

so that (because $[p(y_1, y_3)] \equiv 0$ for $y_1 > 0$)

$$\begin{aligned} p'(\mathbf{x},\omega) &\approx \frac{-i\kappa_0 \sin\psi \sin\theta \mathrm{e}^{i\kappa_0|\omega|}}{4\pi|\mathbf{x}|}\int_{-\infty}^{\infty} dy_3 \int_{-\infty}^{\infty} [p(y_1, y_3)]\mathrm{e}^{-i\kappa_0\mathbf{x}\cdot\mathbf{y}/|\mathbf{x}|}\, dy_1 \\ &= \frac{-\pi i\kappa_0 \sin\psi \sin\theta}{|\mathbf{x}|}[\hat{p}(\kappa_0 x_1/|\mathbf{x}|, \kappa_0 x_3/|\mathbf{x}|)|)]\mathrm{e}^{i\kappa_0|\mathbf{x}|}, \quad |\mathbf{x}| \to \infty, \end{aligned} \tag{14}$$

where

$$[\hat{p}(k_1, k_3)] = \frac{1}{(2\pi)^2}\int_{-\infty}^{\infty} dy_3 \int_{-\infty}^{\infty} [p(y_1, y_3)]\mathrm{e}^{-i(k_1 y_1 + k_3 y_3)}\, dy_1. \tag{15}$$

The first line of (14) implies that the principal contribution to the integral is from those components of $[p(y_1, y_3)]$ with length scales $\sim \mathrm{O}(1/\kappa_0)$. In other words, a correct evaluation of the integral requires the retention of phase information in $[p]$ characterizing fluctuations in the surface pressure over distances of the order of the acoustic wavelength, which typically exceeds the scale of the hydrodynamic motions by a factor $1/M \gg 1$. In this integral phase interference with the exponential factor $\mathrm{e}^{-i\kappa_0\mathbf{x}\cdot\mathbf{y}/|\mathbf{x}|}$ is responsible for correcting the directivity of the sound from that of a free field dipole $\sim \sin\psi \sin\theta \equiv \cos\Theta$ (Θ being the angle between $\mathbf{x}/|\mathbf{x}|$ and the x_2-axis) orientated normal to the airfoil, to $\sin^{\frac{1}{2}}\psi \sin(\theta/2)$, which conforms to the rigid body surface condition ($\partial p'/\partial x_n = 0$) in the far field.

If an attempt is made to approximate the surface pressure jump $[p(y_1, y_3)]$ in Curle's formula (12) by its value for incompressible flow, it would be equivalent to setting

$$[\hat{p}(\kappa_0 x_1/|\mathbf{x}|, \kappa_0 x_3/|\mathbf{x}|)|)] \approx [\hat{p}(0,0)] = \frac{1}{(2\pi)^2}\int_{-\infty}^{\infty} dy_3 \int_{-\infty}^{0} [p(y_1, y_3)]\, dy_1 \equiv \frac{F(\omega)}{(2\pi)^2},$$

in (14), where $F(\omega)$ is the net normal force exerted on the fluid by the half-plane. This force may be determined exactly from the solution (6) to be given by

$$F(\omega) = -2\pi i \int_{-\infty}^{\infty} \frac{p_s(k_1, 0, \omega)\sqrt{\kappa_0 + k_1}}{\sqrt{\kappa_0}(k_1 - i0)}\, dk_1. \tag{16}$$

It is unbounded in the incompressible limit in which $\kappa_o \to 0$, and cannot be reliably computed at low Mach numbers by a numerical simulation of the flow, being determined by the unsteady surface pressures over a distance from the edge of the order of the acoustic wavelength.

A correct prediction of the edge noise from Curle's formula is possible only when the surface pressures are known within the acoustic domain. To use (14), $[\hat{p}(\kappa_o x_1/|\mathbf{x}|, \kappa_o x_3/|\mathbf{x}|)|)]$ must be evaluated from the exact formula (6), in the form

$$\left[\hat{p}\left(\frac{\kappa_o x_1}{|\mathbf{x}|}, \frac{\kappa_o x_3}{|\mathbf{x}|}\right)\right] = \frac{-1}{2\sqrt{2\kappa_o}\pi i \sin^{\frac{1}{2}}\psi \cos(\theta/2)} \int_{-\infty}^{\infty} \frac{\sqrt{\kappa_o \sin\psi + k_1}}{(\kappa_o x_1/|\mathbf{x}| - k_1)} \; p_s(k_1, \kappa_o x_3/|\mathbf{x}|, \omega) dk_1, \tag{17}$$

whose use in (14) leads directly to (8).

2.3 Kirchhoff integral representation

The scattered pressure $p'(\mathbf{x}, \omega)$ of §2.1, satisfies the Helmholtz equation (4) everywhere. By introducing a Green's function $G(\mathbf{x}, \mathbf{y}, \omega)$, which is *any* solution of

$$(\nabla^2 + \kappa_o^2) G = \delta(\mathbf{x} - \mathbf{y}) \tag{18}$$

with *outgoing* wave behavior, $p'(\mathbf{x}, \omega)$ may be represented by the following Kirchhoff integral over S [24]

$$p'(\mathbf{x}, \omega) = \oint_S \left(G(\mathbf{x}, \mathbf{y}, \omega) \frac{\partial p'}{\partial y_n}(\mathbf{y}, \omega) - p'(\mathbf{y}, \omega) \frac{\partial G}{\partial y_n}(\mathbf{x}, \mathbf{y}, \omega) \right) d\mathrm{S}(\mathbf{y}), \tag{19}$$

where the normal derivatives $\partial/\partial y_n$ are directed into the fluid. This equation determines the scattered sound provided p' and $\partial p'/\partial y_n$ are known on S. However, for an arbitrary choice of the Green's function $G(\mathbf{x}, \mathbf{y}, \omega)$, and for the reasons discussed above for Curle's equation, acceptable predictions of the sound are possible only if the variations of p' and $\partial p'/\partial y_n$ on S are specified correctly over length scales comparable to the acoustic wavelengths.

For example, one might attempt to express the radiation entirely in terms of the surface pressure (already determined, say, by means of a subsidiary calculation valid in the neighborhood of the edge) by using a 'pressure release' Green's function that vanishes on S. The first term in the integrand of (19) is then absent, and $p'(\mathbf{x}, \omega) = -\oint_S p'(\mathbf{y}, \omega) \partial G(\mathbf{x}, \mathbf{y}, \omega)/\partial y_n d\mathrm{S}(\mathbf{y})$ would be an *exact* representation of the sound. But, if $p'(\mathbf{y}, \omega)$ in the integrand is known only in an incompressible approximation, the

predicted behavior of $p'(\mathbf{x},\omega)$ at large distances from the edge would be governed by the behavior of $G(\mathbf{x},\mathbf{y},\omega)$ as $|\mathbf{x}| \to \infty$, and the far field scattered pressure would therefore be predicted to *vanish* on S, whereas for a rigid surface $|p'(\mathbf{x},\omega)|$ actually assumes its largest values there! In order for this latter behavior to be predicted, sufficient *phase* information, characterizing changes in $p'(\mathbf{y},\omega)$ on S over distances of the order of the acoustic wavelength, must be included to ensure that a correct estimate is obtained for the asymptotic behavior of the integral (19) as $|\mathbf{x}| \to \infty$. This requirement is equivalent to the correction of the free field *dipole* directivity ($\cos\Theta \equiv \sin\psi \sin\theta$) of (14) brought about by the use of the exact formula (17) for $[p]$ in (12).

The need for such detailed phase information in the prescribed boundary values of p' and $\partial p'/\partial y_n$ can be avoided by using a Green's function that already satisfies the relevant boundary conditions on S. It can then be expected that surface values calculated from an incompressible model of the flow will be sufficient to determine the far field sound at low Mach numbers. For the rigid half-plane the Green's function should have vanishing normal derivative on S (reciprocity actually implies that $\partial G/\partial x_n = 0$, $\partial G/\partial y_n = 0$ respectively on $x_1 < 0$, $x_2 = 0$ and $y_1 < 0$, $y_2 = 0$). Then the second term in the integrand of (19) is absent, and condition (3) gives

$$\begin{aligned} p'(\mathbf{x},\omega) &= -\oint_{\mathrm{S}} \frac{\partial p_{\mathrm{I}}}{\partial y_n}(y_1,0,y_3,\omega) G(\mathbf{x},\mathbf{y};\omega) d\mathrm{S}(\mathbf{y}). \\ &= -\int_{-\infty}^{\infty} dy_3 \int_{-\infty}^{0} \frac{\partial p_{\mathrm{I}}}{\partial y_2}(y_1,0,y_3,\omega) \Big[G(\mathbf{x},\mathbf{y},\omega)\Big]\, dy_1 \end{aligned} \tag{20}$$

where

$$\Big[G(\mathbf{x},\mathbf{y},\omega)\Big] = G(\mathbf{x},y_1,+0,y_3,\omega) - G(\mathbf{x},y_1,-0,y_3,\omega) \tag{21}$$

is the jump in the value of G across the half-plane.

The integrals in (20) may be evaluated by taking $\partial p_{\mathrm{I}}/\partial y_2$ to have its value when compressibility is ignored, provided that those turbulence eddies responsible for the edge noise are always very much closer than an acoustic wavelength from the edge, which is always the case at sufficiently small Mach numbers. It then becomes appropriate to expand Green's function in terms of the nondimensional source distance $\kappa_o\sqrt{y_1^2+y_2^2}$ ($\sim \sqrt{y_1^2+y_2^2}$/acoustic wavelength) from the edge. When the observation point $\mathbf{x}$ is in the acoustic far field we find [25]

$$G(\mathbf{x},\mathbf{y},\omega) = G_0(\mathbf{x},\mathbf{y},\omega) + G_1(\mathbf{x},\mathbf{y},\omega) + \ldots, \tag{22}$$

where, for $|\mathbf{x} - y_3\mathbf{i}_3| \to \infty$ and $\kappa_o\sqrt{y_1^2 + y_2^2} \ll 1$,

$$G_0(\mathbf{x},\mathbf{y},\omega) = \frac{-1}{4\pi|\mathbf{x} - y_3\mathbf{i}_3|}\mathrm{e}^{i\kappa_o|\mathbf{x}-y_3\mathbf{i}_3|}, \quad G_1(\mathbf{x},\mathbf{y},\omega) = \frac{-1}{\pi\sqrt{2\pi i}}\frac{\sqrt{\kappa_o}\varphi^*(\mathbf{x})\varphi^*(\mathbf{y})}{|\mathbf{x} - y_3\mathbf{i}_3|^{3/2}}\mathrm{e}^{i\kappa_o|\mathbf{x}-y_3\mathbf{i}_3|}. \tag{23}$$

$\mathbf{i}_3$ is a unit vector parallel to the x_3-axis (the edge), and the function

$$\varphi^*(\mathbf{x}) = \sqrt{r}\sin(\theta/2) \equiv \sqrt{|\mathbf{x}|}\sin^{\frac{1}{2}}\psi\sin(\theta/2) \tag{24}$$

is equivalent to the velocity potential of incompressible flow around the edge (in the anticlockwise direction) expressed in terms of polar coordinates $(x_1, x_2) = r(\cos\theta, \sin\theta)$. The component G_0 represents the radiation from a point source at $\mathbf{y}$ when scattering by the half-plane is neglected. The component G_1 provides the first correction due to the presence of the half-plane, and (since $[G_0] \equiv 0$) gives the leading approximation to the edge noise when used in (20).

By introducing the representation (5) of p_{I} in terms of the blocked pressure, we find, using (23) in (20),

$$\begin{aligned} p'(\mathbf{x},\omega) &\approx \frac{\sqrt{2\kappa_0}\sin^{\frac{1}{2}}\psi\sin(\theta/2)\mathrm{e}^{i\kappa_0|\mathbf{x}|}}{\pi\sqrt{\pi i}|\mathbf{x}|}\int_{-\infty}^{\infty}dy_3\int_{-\infty}^{0}|y_1|^{\frac{1}{2}}\frac{\partial p_{\mathrm{I}}}{\partial y_2}(y_1,0,y_3)dy_3 \\ &= \frac{-\sqrt{i\kappa_0}\sin^{\frac{1}{2}}\psi\sin(\theta/2)\mathrm{e}^{i\kappa_0|\mathbf{x}|}}{\pi\sqrt{2\pi}|\mathbf{x}|}\int_{-\infty}^{\infty}\gamma(k)p_s(\mathbf{k},\omega)d^2\mathbf{k}\int_{-\infty}^{\infty}\mathrm{e}^{ik_3y_3}dy_3\int_{-\infty}^{0}|y_1|^{\frac{1}{2}}\mathrm{e}^{ik_1y_1}dy_1. \end{aligned} \tag{25}$$

The y_3-integral equals $2\pi\delta(k_3)$; the y_1-integral must be treated as the Fourier transform of a generalized function [26], and evaluated by integration by parts, when it is found to be equal to

$$\frac{-1}{2|k_1|}\sqrt{\frac{\pi i}{k_1 + i0}}.$$

When compressible effects in the specification of the blocked pressure are neglected, it may be assumed that $\kappa_0 \ll k_1$ for all relevant values of k_1 in the wavenumber integral. Then $\gamma(k) \to i|k_1|$ and (25) reduces to precisely the low Mach number approximation (9) obtained previously by diffraction theory.

3. ARBITRARY TRAILING EDGE GEOMETRY

3.1 Vortex sound theory

The diffraction theory of §2.1 is conveniently extended to an airfoil of finite thickness (Figure 2) by means of the theory of vortex sound [25], in which the total enthalpy B, rather than the pressure or density, is taken as the fundamental acoustic variable. When the mean flow Mach number is small enough that the convection of sound may be ignored, and when the mean fluid density is constant,

$$\left(\frac{1}{c_0^2}\frac{\partial^2}{\partial t^2} - \nabla^2\right) B = \mathrm{div}(\boldsymbol{\Omega} \wedge \mathbf{v}), \tag{26}$$

where $\boldsymbol{\Omega}(\mathbf{x}, t) = \mathrm{curl}\ \mathbf{v}$ is the vorticity. In those regions where the unsteady motion is irrotational ($\boldsymbol{\Omega} = \mathbf{0}$) yet still, perhaps, predominantly nonlinear, it can be described by a velocity potential $\phi(\mathbf{x}, t)$, say, which satisfies $B = -\partial\phi/\partial t$. In the acoustic far field the small amplitude pressure fluctuations are determined in terms of B by the linear relation

$$\frac{p'(\mathbf{x}, t)}{\rho_0} \approx -\frac{\partial\phi}{\partial t} \equiv B(\mathbf{x}, t). \tag{27}$$

Equation (26) relates fluctuations in B to the vorticity and velocity. The radiation condition requires the solution to have outgoing wave behavior, and for each Fourier component of frequency ω it can be expressed as the sum of a Kirchhoff integral representing a contribution from the surface S of the airfoil (as in (19)) plus the direct radiation from the vortex sources:

$$B(\mathbf{x}, \omega) = \oint_S \left(\frac{\partial B}{\partial y_n}(\mathbf{y}, \omega) G(\mathbf{x}, \mathbf{y}, \omega) - B(\mathbf{y}, \omega)\frac{\partial G}{\partial y_n}(\mathbf{x}, \mathbf{y}, \omega)\right) d\mathrm{S}(\mathbf{y})$$

$$- \int G(\mathbf{x}, \mathbf{y}, \omega)\Big(\mathrm{div}(\boldsymbol{\Omega} \wedge \mathbf{v})(\mathbf{y}, \omega)\Big) d^3\mathbf{y}, \tag{28}$$

where $G(\mathbf{x}, \mathbf{y}, \omega)$ is an outgoing solution of (18).

Let the Green's function satisfy the rigid surface condition $\partial G/\partial y_n = 0$ on S, and use the divergence theorem to transform the volume integral in (28) as follows:

$$\int G\,\mathrm{div}(\boldsymbol{\Omega} \wedge \mathbf{v}) d^3\mathbf{y} = -\oint_S G(\boldsymbol{\Omega} \wedge \mathbf{v}) \cdot \mathbf{n} d\mathrm{S}(\mathbf{y}) - \int (\boldsymbol{\Omega} \wedge \mathbf{v}) \cdot \nabla G d^3\mathbf{y},$$

where the unit normal $\mathbf{n}$ on S is directed into the fluid. Then

$$B(\mathbf{x}, \omega) = \oint_S G(\mathbf{x}, \mathbf{y}, \omega)\left(\frac{\partial B}{\partial y_n} + (\boldsymbol{\Omega} \wedge \mathbf{v}) \cdot \mathbf{n}\right)(\mathbf{y}, \omega)\, d\mathrm{S}(\mathbf{y}) + \int \frac{\partial G}{\partial \mathbf{y}}(\mathbf{x}, \mathbf{y}, \omega) \cdot \Big(\boldsymbol{\Omega} \wedge \mathbf{v}\Big)(\mathbf{y}, \omega) d^3\mathbf{y}. \tag{29}$$

Very close to S viscous effects are dominated by shear stresses, and the momentum equation can be taken in Crocco's form

$$\partial \mathbf{v}/\partial t + \nabla B = -\boldsymbol{\Omega} \wedge \mathbf{v} - \nu \operatorname{curl} \boldsymbol{\Omega}$$

where ν is the kinematic viscosity. But $\mathbf{v} \equiv \mathbf{0}$ on S when the airfoil is rigid and at rest. Hence (29) becomes

$$B(\mathbf{x},\omega) = \int \frac{\partial G}{\partial \mathbf{y}}(\mathbf{x},\mathbf{y},\omega) \cdot \big(\boldsymbol{\Omega} \wedge \mathbf{v}\big)(\mathbf{y},\omega) d^3\mathbf{y} - \nu \oint_{\mathrm{S}} G(\mathbf{x},\mathbf{y},\omega) \operatorname{curl} \boldsymbol{\Omega} \cdot \mathbf{n} d\mathrm{S}(\mathbf{y}),$$

and the identity $G\operatorname{curl} \boldsymbol{\Omega} \equiv \operatorname{curl}(G\boldsymbol{\Omega}) + \boldsymbol{\Omega} \wedge \nabla G$ and the divergence theorem then yield

$$B(\mathbf{x},\omega) = \int \frac{\partial G}{\partial \mathbf{y}}(\mathbf{x},\mathbf{y},\omega) \cdot \big(\boldsymbol{\Omega} \wedge \mathbf{v}\big)(\mathbf{y},\omega) d^3\mathbf{y} - \nu \oint_{\mathrm{S}} \boldsymbol{\Omega}(\mathbf{y},\omega) \wedge \frac{\partial G}{\partial \mathbf{y}}(\mathbf{x},\mathbf{y},\omega) \cdot \mathbf{n}\, d\mathrm{S}(\mathbf{y}). \quad (30)$$

The surface integral is the contribution to the radiation from the unsteady skin friction on S, and is usually ignored when the Reynolds number is large.

The remaining integrals can be evaluated at low Mach numbers by expanding the Green's function in the form (22), provided the characteristic acoustic wavelength is much larger than the airfoil thickness. The principal contribution is from $G_1(\mathbf{x},\mathbf{y},\omega)$ which, however, must now be taken in the form [17]

$$G_1(\mathbf{x},\mathbf{y},\omega) = \frac{-1}{\pi\sqrt{2\pi i}} \frac{\sqrt{\kappa_o}\varphi^*(\mathbf{x})\Phi^*(\mathbf{y})}{|\mathbf{x} - y_3\mathbf{i}_3|^{3/2}} \mathrm{e}^{i\kappa_o|\mathbf{x}-y_3\mathbf{i}_3|}, \quad (31)$$

where the potential $\varphi^*(\mathbf{y}) \equiv \varphi^*(y_1, y_2)$ of (23) is replaced by $\Phi^*(\mathbf{y}) \equiv \Phi^*(y_1, y_2, y_3)$, which describes incompressible potential flow around the edge of the airfoil, such that

$$\Phi^*(y_1, y_2, y_3) \to \varphi^*(y_1, y_2), \quad \text{as } \sqrt{y_1^2 + y_2^2} \to \infty.$$

We now find, in the acoustic far field,

$$p'(\mathbf{x},\omega) \approx \frac{-\rho_o \kappa_o^{\frac{1}{2}} \sin^{\frac{1}{2}}\psi \sin(\theta/2) \mathrm{e}^{i\kappa_o|\mathbf{x}|}}{\pi\sqrt{2\pi i}|\mathbf{x}|} \Big\{ \int \frac{\partial \Phi^*(\mathbf{y})}{\partial \mathbf{y}} \cdot \big(\boldsymbol{\Omega} \wedge \mathbf{v}\big)(\mathbf{y},\omega) d^3\mathbf{y}$$

$$- \nu \oint_{\mathrm{S}} \boldsymbol{\Omega}(\mathbf{y},\omega) \wedge \frac{\partial \Phi^*(\mathbf{y})}{\partial \mathbf{y}} \cdot \mathbf{n}\, d\mathrm{S}(\mathbf{y}) \Big\}, \quad |\mathbf{x}| \to \infty. \quad (32)$$

The radiated sound automatically satisfies the rigid surface boundary condition on the distant parts of the airfoil, so that the vorticity $\boldsymbol{\Omega}$ and the velocity $\mathbf{v}$ in the integrands can be approximated by their values calculated for incompressible flow near the edge of the airfoil. The term in the brace brackets of (32) is proportional to the net normal force $F(\omega)$

exerted on the fluid by the airfoil. As noted in §2.2, this force increases in proportion to the square root of the acoustic wavelength; in the present notation it is given by [17]

$$F(\omega) \approx 2\rho_o\sqrt{\frac{i}{\pi\kappa_o}}\Big\{\int \frac{\partial\Phi^*(\mathbf{y})}{\partial\mathbf{y}}\cdot\big(\mathbf{\Omega}\wedge\mathbf{v}\big)(\mathbf{y},\omega)d^3\mathbf{y} - \nu\oint_S \mathbf{\Omega}(\mathbf{y},\omega)\wedge\frac{\partial\Phi^*(\mathbf{y})}{\partial\mathbf{y}}\cdot\mathbf{n}\,dS(\mathbf{y})\Big\}.$$

3.2 Diffraction theory

The evaluation of (32) requires the vorticity and velocity fields to be known in the neighborhood of the edge. An alternative representation of the sound, which is analogous to (9) for the flat-plate airfoil, can be derived by consideration of the diffraction theory of §2.1. We shall not, however, assume the boundary layer turbulence to be frozen during convection past the edge, but will introduce an 'incident' disturbance B_I which is defined to be the exact solution of equation (26) *in the absence of the airfoil* when the vorticity $\mathbf{\Omega}$ and velocity $\mathbf{v}$ on the right of (26) have their exact values.

To calculate B_I the interior of the airfoil is imagined to be replaced by fluid with no acoustic sources, wherein the actual motion is determined by the source distribution $\mathbf{\Omega}\wedge\mathbf{v}$ outside S. Then, for each component of frequency ω,

$$B_I(\mathbf{x},\omega) = \frac{1}{4\pi}\int_V \frac{e^{i\kappa_o|\mathbf{x}-\mathbf{y}|}}{|\mathbf{x}-\mathbf{y}|}\frac{\partial}{\partial\mathbf{y}}\cdot\big(\mathbf{\Omega}\wedge\mathbf{v}\big)(\mathbf{y},\omega)d^3\mathbf{y}, \tag{33}$$

where V is the fluid volume outside S. When compressibility is neglected in the source region near the edge

$$\frac{\partial}{\partial\mathbf{y}}\cdot\big(\mathbf{\Omega}\wedge\mathbf{v}\big) \equiv \frac{\partial^2 v_i v_j}{\partial y_i\partial y_j} - \nabla^2\left(\frac{1}{2}v^2\right), \tag{34}$$

and therefore, because $\mathbf{v}$ vanishes on S, the acoustic pressure $p_I \approx \rho_o B_I$ in the far field corresponds to the quadrupole field

$$p_I(\mathbf{x},\omega) \approx \frac{-\kappa_o^2 e^{i\kappa_o|\mathbf{x}|}}{4\pi|\mathbf{x}|}\left(\frac{x_i x_j}{|\mathbf{x}|^2} - \frac{1}{2}\delta_{ij}\right)\int_V \rho_o(v_i v_j)(\mathbf{y},\omega)d^3\mathbf{y}, \quad |\mathbf{x}|\to\infty, \tag{35}$$

which is negligible compared to the edge generated sound.

The effect of the airfoil is calculated by setting

$$B(\mathbf{x},t) = B'(\mathbf{x},t) + B_I(\mathbf{x},t), \tag{36}$$

where B' satisfies the *homogeneous* form of (26) (no sources). B' and B_I are related by the no-slip boundary condition on S, which the momentum equation gives in the form

$$\nabla B' + \nabla B_I = -\nu\,\mathrm{curl}\,\mathbf{\Omega} \quad \text{on S.} \tag{37}$$

Thus, when Kirchhoff's formula (19) is used (with p' replaced by B'), we find

$$B'(\mathbf{x},\omega) = -\oint_{\mathrm{S}} G(\mathbf{x},\mathbf{y},\omega)\left(\frac{\partial B_{\mathrm{I}}}{\partial y_n} + \nu \mathrm{curl}\,\boldsymbol{\Omega}\cdot\mathbf{n}\right)(\mathbf{y},\omega)d\mathrm{S}(\mathbf{y}), \tag{38}$$

provided $\partial G/\partial y_n = 0$ on S.

Taking the low Mach number expansion of the Green's function, the leading order term of which is given by (31), we find

$$p'(\mathbf{x},\omega) \approx \frac{\rho_{\mathrm{o}}\kappa_{\mathrm{o}}^{\frac{1}{2}}\sin^{\frac{1}{2}}\psi\sin(\theta/2)\mathrm{e}^{i\kappa_{\mathrm{o}}|\mathbf{x}|}}{\pi\sqrt{2\pi i}|\mathbf{x}|}\oint_{\mathrm{S}}\left(\Phi^*(\mathbf{y})\frac{\partial B_{\mathrm{I}}}{\partial y_n}(\mathbf{y},\omega) + \nu\boldsymbol{\Omega}(\mathbf{y},\omega)\wedge\frac{\partial\Phi^*(\mathbf{y})}{\partial\mathbf{y}}\cdot\mathbf{n}\right)d\mathrm{S}(\mathbf{y}),$$

$$|\mathbf{x}|\to\infty, \tag{39}$$

where the integrand is to be evaluated using incompressible approximations for $\partial B_{\mathrm{I}}/\partial y_n$ and $\boldsymbol{\Omega}$.

This prediction of the far field sound is identical to that given by (32). Indeed, because $\partial\Phi^*/\partial y_n = 0$ on S, the following relations are readily seen to transform the first term of the integral of (39) into the corresponding term in (32):

$$\mathrm{div}\left(\Phi^*\nabla B_{\mathrm{I}} - B_{\mathrm{I}}\nabla\Phi^*\right) \equiv \Phi^*\nabla^2 B_{\mathrm{I}} - B_{\mathrm{I}}\nabla^2\Phi^* \equiv \Phi^*\nabla^2 B_{\mathrm{I}} \approx -\Phi^*\mathrm{div}\left(\boldsymbol{\Omega}\wedge\mathbf{v}\right),$$

where the final approximation follows from the incompressible limit of equation (26).

By setting $\kappa_{\mathrm{o}} = 0$ in (33) we derive a local incompressible representation of B_{I}, from which it is readily deduced that

$$\nabla B_{\mathrm{I}} + \boldsymbol{\Omega}\wedge\mathbf{v} = \mathrm{curl}\int_{\mathrm{V}}\frac{\mathrm{curl}\,(\boldsymbol{\Omega}\wedge\mathbf{v})d^3\mathbf{y}}{4\pi|\mathbf{x}-\mathbf{y}|} \equiv -\mathrm{curl}\int_{\mathrm{V}}\left(\frac{\partial\boldsymbol{\Omega}}{\partial t} - \nu\nabla^2\boldsymbol{\Omega}\right)\frac{d^3\mathbf{y}}{4\pi|\mathbf{x}-\mathbf{y}|}, \tag{40}$$

where use has been made of the curl of the incompressible momentum equation: $\partial\mathbf{v}/\partial t + \nabla B = -\boldsymbol{\Omega}\wedge\mathbf{v} - \nu\mathrm{curl}\,\boldsymbol{\Omega}$. In the viscous sublayer, close to the surface of the airfoil, the motion becomes *linear* and

$$\tfrac{\partial\boldsymbol{\Omega}}{\partial t} - \nu\nabla^2\boldsymbol{\Omega} \approx \mathbf{0}.$$

Outside the sublayer viscous diffusion is negligible, and $\nu\nabla^2\boldsymbol{\Omega}$ may be discarded from the integrand. Hence, we can introduce an 'upwash velocity' $\mathbf{v}_{\mathrm{I}}$ by means of the Biot-Savart formula [27]

$$\mathbf{v}_{\mathrm{I}}(\mathbf{x},t) = \mathrm{curl}\int_{\mathrm{V}_\delta}\frac{\boldsymbol{\Omega}(\mathbf{y},t)d^3\mathbf{y}}{4\pi|\mathbf{x}-\mathbf{y}|}, \tag{41}$$

where the integration is confined to the boundary layer vorticity in the nonlinear region V_δ *outside* the viscous sublayer. On S and within the volume of the airfoil, $\partial \mathbf{v}_I/\partial t = -\nabla B_I$, in terms of which the far field sound becomes

$$p'(\mathbf{x},\omega) \approx \frac{\rho_o \omega \sqrt{i\kappa_o} \sin^{\frac{1}{2}}\psi \sin(\theta/2) e^{i\kappa_o|\mathbf{x}|}}{\pi\sqrt{2\pi}|\mathbf{x}|} \oint_S \Phi^*(\mathbf{y}) v_{In}(\mathbf{y},\omega) dS(\mathbf{y}), \quad |\mathbf{x}| \to \infty, \tag{42}$$

where $v_{In} = \mathbf{v}_I \cdot \mathbf{n}$. Note that in applications to problems in which, for the purpose of calculation, the whole motion is regarded as inviscid, the definition (41) makes it clear that in calculating $\mathbf{v}_I$ the *bound vorticity* on S must be excluded from the integral.

Equation (42) generalizes the Chase-Chandiramani formula (9) for the flat plate airfoil, to which it reduces when S is a semi-infinite half-plane. To see this it is necessary to note that, in an incompressible approximation of the flow near the edge, the incident pressure p_I of (5) is the solution of

$$\nabla^2 p_I = -\rho_o \frac{\partial^2 v_i v_j}{\partial x_i \partial x_j} \equiv -\rho_o \mathrm{div}(\boldsymbol{\Omega} \wedge \mathbf{v}) - \rho_o \nabla^2 \left(\frac{1}{2} v^2\right)$$

when the presence of the airfoil is ignored. Hence $B_I = p_I/\rho_o + \frac{1}{2}v^2$, where $\mathbf{v}$ is the fluid velocity, which vanishes on and within S where, accordingly,

$$\frac{\partial \mathbf{v}_I}{\partial t} = -\nabla B_I \equiv \frac{-1}{\rho_o} \nabla p_I. \tag{43}$$

When v_{In} in (41) is replaced by $(1/i\rho_o\omega)\partial p_I/\partial y_n$ the first line of (25) is recovered, leading to our previous result (9).

For a time-stationary random flow past the edge we can introduce a frequency correlation function $\mathcal{R}_{vv}(\mathbf{y},\mathbf{y}',\omega)$ that satisfies

$$\langle v_{In}(\mathbf{y},\omega) v_{In}^*(\mathbf{y}',\omega')\rangle = \mathcal{R}_{vv}(\mathbf{y},\mathbf{y}',\omega)\delta(\omega-\omega'). \tag{44}$$

The acoustic pressure frequency spectrum (defined as for (11)) then becomes

$$\Phi(\mathbf{x},\omega) \approx \frac{\rho_o^2 \omega^3 \sin\psi \sin^2(\theta/2)}{\pi^3 c_o |\mathbf{x}|^2} \oint_S \mathcal{R}_{vv}(\mathbf{y},\mathbf{y}',\omega)\Phi^*(\mathbf{y})\Phi^*(\mathbf{y}') dS(\mathbf{y}) dS(\mathbf{y}'), \quad \omega > 0. \tag{45}$$

3.3 Two-dimensional source distributions

We record here the modifications of formulae given above when the aeroacoustic sources and trailing edge can be regarded as two-dimensional, with no dependence on the spanwise coordinate x_3. At very small Mach numbers, the dominant component of the Green's function whose normal derivative vanishes on S is obtained by integrating (31) over $-\infty < y_3 < \infty$. When $\mathbf{x}$ lies in the acoustic far field the integration can be performed by the method of stationary phase, which yields [5]

$$G_1(\mathbf{x},\mathbf{y},\omega) \approx -\frac{\varphi^*(\mathbf{x})\Phi^*(\mathbf{y})}{\pi|\mathbf{x}|}\,\mathrm{e}^{i\kappa_o|\mathbf{x}|} \equiv \frac{-\sin(\theta/2)\Phi^*(\mathbf{y})}{\pi|\mathbf{x}|^{\frac{1}{2}}}\,\mathrm{e}^{i\kappa_o|\mathbf{x}|}\,, \tag{46}$$

where now $\mathbf{x} = (x_1, x_2),\ \mathbf{y} = (y_1, y_2)$.

Thus, the two-dimensional analog of (32) is the *cylindrically spreading* wave field

$$p'(\mathbf{x},\omega) \approx \frac{-\rho_o \sin(\theta/2)\mathrm{e}^{i\kappa_o|\mathbf{x}|}}{\pi|\mathbf{x}|^{\frac{1}{2}}}\Big\{\int \frac{\partial\Phi^*(\mathbf{y})}{\partial\mathbf{y}}\cdot\big(\mathbf{\Omega}\wedge\mathbf{v}\big)(\mathbf{y},\omega)d^2\mathbf{y} - \nu\oint_S \mathbf{\Omega}(\mathbf{y},\omega)\wedge\frac{\partial\Phi^*(\mathbf{y})}{\partial\mathbf{y}}\cdot\mathbf{n}\,ds(\mathbf{y})\Big\},\quad |\mathbf{x}|\to\infty,$$

where $ds > 0$ is the line element on the airfoil profile in the x_1x_2-plane. This has the simple time-domain form

$$p'(\mathbf{x},t) \approx \frac{-\rho_o \sin(\theta/2)}{\pi|\mathbf{x}|^{\frac{1}{2}}}\Big[\int \frac{\partial\Phi^*(\mathbf{y})}{\partial\mathbf{y}}\cdot\big(\mathbf{\Omega}\wedge\mathbf{v}\big)(\mathbf{y},t)d^2\mathbf{y} - \nu\oint_S \mathbf{\Omega}(\mathbf{y},t)\wedge\frac{\partial\Phi^*(\mathbf{y})}{\partial\mathbf{y}}\cdot\mathbf{n}\,ds(\mathbf{y})\Big],$$

which decays in amplitude like $1/|\mathbf{x}|^{\frac{1}{2}}$ at large distances from the edge, and where the term in the square brackets [ ] is evaluated at the retarded time $t - |\mathbf{x}|/c_o$. For inviscid (or very high Reynolds number) flow we can take

$$p'(\mathbf{x},t) \approx \frac{-\rho_o \sin(\theta/2)}{\pi|\mathbf{x}|^{\frac{1}{2}}}\Big[\int \frac{\partial\Phi^*(\mathbf{y})}{\partial\mathbf{y}}\cdot\big(\mathbf{\Omega}\wedge\mathbf{v}\big)(\mathbf{y},t)d^2\mathbf{y}\Big]. \tag{47}$$

Similarly, the diffraction theory formulae (38) and (42) have the corresponding representations

$$\begin{aligned} p'(\mathbf{x},t) &\approx \frac{\rho_o \sin(\theta/2)}{\pi|\mathbf{x}|^{\frac{1}{2}}}\oint_S \Phi^*(\mathbf{y})\left[\frac{\partial B_I}{\partial y_n}(\mathbf{y},t)\right]ds \\ &\equiv -\frac{\rho_o \sin(\theta/2)}{\pi|\mathbf{x}|^{\frac{1}{2}}}\oint_S \Phi^*(\mathbf{y})\left[\frac{\partial v_{In}}{\partial t}(\mathbf{y},t)\right]ds,\quad |\mathbf{x}|\to\infty, \end{aligned} \tag{48}$$

where the skin friction contribution has been discarded.

4. ROUNDED TRAILING EDGE

Rounded or bevelled trailing edges, of the type depicted in Figure 3a, are frequently used in experimental studies of trailing edge noise at low Mach numbers [1, 27, 28]. The simplified geometry is suitable for validating numerical methods for edge noise prediction. When the Mach number is small enough for the edge flow to be regarded as incompressible, it is necessary to be able to determine numerically the velocity and vorticity distributions near the edge, or equivalently, the 'upwash' velocity v_{In}. In this section the procedure is illustrated for a highly simplified two-dimensional edge flow that can be treated analytically.

4.1 Formulation

A line (or 'point') vortex of circulation Γ is parallel to the edge of the airfoil and convects in the mean flow. Except very close to the edge, the airfoil has uniform thickness h and its 'upper' and 'lower' surfaces coincide with the planes $x_2 = \pm\frac{1}{2}h$. The upper surface is rounded over the interval $-\ell < x_1 < 0$, and meets the lower surface at A: $x_1 = 0$, $x_2 = -\frac{1}{2}h$ (Figure 3a). At large distances from the airfoil the mean flow is at speed U in the x_1-direction, and the mean circulation around the airfoil is assumed to be adjusted to make A a stagnation point.

Viscosity is ignored in the body of the fluid, so that the two-dimensional motion of the vortex can be determined by mapping the fluid region bounded by the airfoil in the complex plane of $z = x_1 + ix_2$ onto the upper half of the ζ-plane. To do this we introduce the complex function

$$f(\zeta,\beta) = -\frac{4}{\pi(1+\beta)^2}\left(\zeta+\frac{\beta-1}{2}\right)\sqrt{\zeta+\beta}\sqrt{\zeta-1}+\frac{1}{\pi}\ln\left[\left(\zeta+\frac{\beta-1}{2}\right)+\sqrt{\zeta+\beta}\sqrt{\zeta-1}\right]$$

$$-\frac{i}{2}-\frac{1}{\pi}\ln\left(\frac{1+\beta}{2}\right), \qquad \beta = \text{constant} > -1. \tag{49}$$

The transformation

$$\frac{z}{h} = f(\zeta,\beta)$$

maps the exterior of the semi-infinite airfoil of uniform *rectangular* cross-section and thickness h shown in Figure 3b onto $\mathrm{Im}\,\zeta > 0$, such that the boundary points C, A, B, D on S correspond respectively to the points C′, A′, B′, D′ on the real ζ-axis.

It may then be verified that the composite transformation

$$\frac{z}{h} = \frac{1}{(1+\alpha)}\big[f(\zeta,1)+\alpha f(\zeta,\beta)\big], \quad \alpha > 0, \quad \beta > +1, \tag{50}$$

where α is a second constant, maps the real ζ-axis onto an airfoil profile S whose upper and lower surfaces coincide with $x_2 = \pm\frac{1}{2}h$ respectively for $\mathrm{Re}\,\zeta < -\beta$ and $\mathrm{Re}\,\zeta > 1$. The interval $-\beta < \mathrm{Re}\,\zeta < -1$ maps into an upper 'rounded' section of the trailing edge (as in Figure 3a) which terminates at $\zeta = -1$ at the top of a vertical end-face ($x_1 = 0$, $-\frac{1}{2}h < x_2 < -\frac{1}{2}h + \Delta$) of thickness Δ, that corresponds to the interval $-1 < \mathrm{Re}\,\zeta < 1$. The constants α and β are determined by the prescribed values of the ratios ℓ/h and Δ/h. For the calculations presented in this chapter we take

$$\alpha = 600, \quad \beta = 86.9370 \tag{51}$$

for which $\ell/h = 4$ and $\Delta/h = 0.0074$. The corresponding airfoil profile is that shown in Figure 3a (because $\Delta \ll h$ the end-face cannot be distinguished).

When the edge A is a stagnation point, the complex velocity potential of mean flow is readily confirmed to be given by

$$w_{\mathrm{m}} = \frac{-Uh}{\pi(1+\alpha)}\left[1 + \frac{4\alpha}{(1+\beta)^2}\right](\zeta - 1)^2, \tag{52}$$

which becomes asymptotically $w_{\mathrm{m}} \approx Uz$ when $|z| \gg h$. The vortex Γ is convected by the mean flow and by the induced velocity field of 'image' vortices in the airfoil. If A is also a stagnation point of the unsteady flow, i.e., if the unsteady Kutta condition is applied there, additional vorticity is shed from A, and will also influence the motion of Γ. We first consider the motion and sound generation in the absence of vortex shedding.

4.2 No vortex shedding

Let $z_{\mathrm{o}}(t)$ denote the complex position of Γ at time t. The velocity potential of the (incompressible) flow produced by Γ is

$$w_\Gamma = \frac{-i\Gamma}{2\pi}\Big\{\ln(\zeta - \zeta_{\mathrm{o}}) - \ln(\zeta - \zeta_{\mathrm{o}}^*)\Big\},$$

where $\zeta_{\mathrm{o}} = \zeta(z_{\mathrm{o}})$ is the image of z_{o} in the ζ-plane, and the asterisk denotes complex conjugate. The complex potential of the velocity component of the motion of Γ produced by image vorticity is obtained by subtracting the 'self potential' $(-i\Gamma/2\pi)\ln(z - z_{\mathrm{o}})$ from w_Γ. The equation of motion of Γ is accordingly obtained in the form

$$\frac{dz_{\mathrm{o}}^*}{dt} = \frac{-i\Gamma}{2\pi}\left[\frac{\zeta_{\mathrm{o}}''}{2\zeta_{\mathrm{o}}'} - \frac{\zeta_{\mathrm{o}}'}{\zeta_{\mathrm{o}} - \zeta_{\mathrm{o}}^*}\right] + \left(\frac{dw_{\mathrm{m}}}{dz}\right)_{\mathrm{o}}, \tag{53}$$

where the suffix 'o' implies evaluation at $z = z_o$, and the primes indicate differentiation with respect to z. This equation must be integrated numerically to determine the path of the vortex, and it is convenient to do this in the ζ-plane, where it is equivalent to

$$\frac{d\zeta_o^*}{dt} = \frac{-i\Gamma\zeta_o'^*}{2\pi}\left[\frac{\zeta_o''}{2\zeta_o'} - \frac{\zeta_o'}{\zeta_o - \zeta_o^*}\right] + \left(\frac{dw_m}{d\zeta}\right)_o |\zeta_o'|^2. \tag{54}$$

The solid curve in Figure 4a depicts the calculated path when the vortex is released at a large distance upstream of the edge, above the airfoil at a stand-off distance $d = \frac{1}{2}h$ from the upper surface. The vortex initially translates along a path parallel to the upper flat surface of the airfoil at speed $U + u$, where

$$u = \frac{\Gamma}{4\pi d}. \tag{55}$$

The results discussed below are obtained for $u = -0.1U$. This corresponds roughly to a typical large fluctuation velocity close to the wall of a turbulent boundary layer [30]. The trajectory shown in Figure 4a was computed (using a fourth order Runge-Kutta scheme [20]) by adjusting the value of ζ_o far upstream of the edge to make the initial stand-off distance d (determined in terms of ζ_o by (50)) equal to $\frac{1}{2}h$. The vortex location is indicated in the figure at different nondimensional times Ut/h, measured from the instant that it crosses $x_1 = 0$.

Two other trajectories are also shown in the figure. The 'frozen' path corresponds to the Chase-Chandiramani approximation [11, 12], in which turbulent structures are assumed to translate past the edge at a uniform mean convection velocity parallel to the airfoil. The position of the vortex on this path has been calculated by taking the uniform convection velocity to be $U + u$ (not U), i.e., its 'exact' value when located above the flat section of the surface of the airfoil. The path labeled 'rdt' is determined by neglecting the influence of image vortices on the motion of Γ, whose equation of motion is now (53) with the omission of the first of the two terms on the right hand side. This corresponds to the approximation of 'rapid distortion theory', where each turbulent element is assumed to convect across an inhomogeneous region at the local mean stream velocity [31, 32]; for the purpose of this illustration it has again been assumed that the mean velocity far from the edge is $U + u$. In all cases, therefore, the vortex passes by the edge at approximately the same speed.

Sound is generated by the vortex principally during its passage past the edge, and can be calculated from either of the formulae (47), (48), by noting that the transformation (50)

implies that

$$\Phi^*(\mathbf{y}) = \mathrm{Re}\left\{-\zeta\sqrt{\frac{h}{\pi(1+\alpha)}\left(1+\frac{4\alpha}{(1+\beta)^2}\right)}\right\}, \tag{56}$$

where ζ is the image of $z = y_1 + iy_2$, and $\mathbf{y} = (y_1, y_2)$.

Now, for a line vortex,

$$\boldsymbol{\Omega} = \Gamma \mathbf{i}_3 \delta\big(\mathbf{y} - \mathbf{x}_\mathrm{o}(t)\big) \quad \text{and} \quad \mathbf{v} = \frac{d\mathbf{x}_\mathrm{o}}{dt}(t), \tag{57}$$

where $\mathbf{x}_\mathrm{o}(t)$ is the vortex location at time t calculated from (53), (54), and we therefore find from (47)

$$p'(\mathbf{x},t) \approx \frac{-\rho_\mathrm{o}\Gamma\sin(\theta/2)}{\pi^{\frac{3}{2}}}\sqrt{\frac{h}{|\mathbf{x}|}}\left(\frac{1+4\alpha/(1+\beta)^2}{1+\alpha}\right)^{\frac{1}{2}} \mathrm{Im}\left[\frac{d\zeta_\mathrm{o}}{dt}\right], \quad |\mathbf{x}| \to \infty, \tag{58}$$

where ζ_o is evaluated at the retarded time $[t] = t - |\mathbf{x}|/c_\mathrm{o}$.

The 'exact' curve in Figure 4b is a nondimensional representation of the pressure signature plotted against $U[t]/h$. Also shown are the corresponding predictions of rapid distortion theory and the frozen approximation. The high frequency components of the sound are generated by scattering at the sharp edge of the airfoil, and the peak radiated pressure occurs in the neighborhood of $[t] = 0$ when the vortex passes close to the edge. In the frozen approximation the contributions to the sound at higher frequencies are reduced because small scale disturbances generated by the vortex, that are responsible for the high frequency sound, decay rapidly as the stand-off distance of the vortex path from the edge A increases.

The sound can also be calculated from the diffraction theory formula (48). To do this, recall that $B_\mathrm{I} = -\partial\phi_\mathrm{I}/\partial t$, where in two-dimensions the 'free space' velocity potential ϕ_I of the vortex is given by

$$\phi_\mathrm{I}(\mathbf{x},t) = \mathrm{Re}\left\{\frac{-i\Gamma}{2\pi}\ln(z - z_\mathrm{o}(t))\right\}, \quad z = x_1 + ix_2.$$

It now follows, using the representation (56) of $\Phi^*(\mathbf{y})$, that

$$p'(\mathbf{x},t) \approx -\frac{\rho_\mathrm{o}\Gamma\sin(\theta/2)}{2\pi^{\frac{5}{2}}}\sqrt{\frac{h}{|\mathbf{x}|}}\left(\frac{1+4\alpha/(1+\beta)^2}{1+\alpha}\right)^{\frac{1}{2}} \mathrm{Re}\left[\frac{dz_\mathrm{o}}{dt}\oint_\mathrm{S}\frac{\zeta\, dz}{(z-z_\mathrm{o})^2}\right], \quad |\mathbf{x}| \to \infty, \tag{59}$$

where the integration is in the *anticlockwise* direction about the contour S of the airfoil in the z-plane, and the square brackets denote evaluation at the retarded time $t - |\mathbf{x}|/c_\mathrm{o}$.

The integrand $\sim O(1/|z|^{\frac{3}{2}})$ as $|z| \to \infty$. The integral may therefore be evaluated by residues by shifting the integration contour to a large circle at infinity, thereby capturing a contribution from the pole at $z = z_0(t)$. This procedure yields (58). Alternatively, (59) can be used to investigate the contributions to the diffraction radiation from the lower and upper surfaces of the airfoil, which are determined by the respective contributions to the integral from the lower surface between $z = -\infty - ih/2$ and $z = -ih/2$ and from the upper, rounded surface between $z = -ih/2$ and $-\infty + ih/2$. These separate integrals have been evaluated numerically, and the corresponding pressures are labelled 'lower surface' and 'upper' in Figure 5 for the conditions of Figure 4, for the case in which the vortex moves along the solid ('exact') path of Figure 4a. The net acoustic pressure is the algebraic sum of these separate contributions.

4.3 Influence of vortex shedding

When the Kutta condition is imposed at the edge A of the airfoil during the passage of Γ, vorticity is shed into the flow and swept downstream. The acoustic radiation consists of the direct sound generated by Γ, considered in §4.2, and the sound generated by the wake. If $u \ll U$, where $u = \Gamma/4\pi d$ is the characteristic induced velocity of the vortex, the trajectory and the acoustic pressure signature of Γ are to a good approximation the same as when the vortex convects at the local mean stream velocity (according to 'rapid distortion theory', see Figure 4). We shall therefore adopt this approximation to examine the influence of the wake, by assuming that both Γ and the shed vorticity convect at the local free stream velocity along undisturbed streamlines of the mean flow. This is equivalent to the linearized approximation of unsteady thin airfoil theory [33, 34], where the airfoil is modelled as a plate of infinitesimal thickness parallel to the mean flow (as in §2), and all perturbation quantities are proportional to the amplitude of an incident 'gust'. In that case, however, both the gust and the wake vorticity convect parallel to the plate at the same, uniform mean stream velocity, and the acoustic pressure generated by the wake turns out to be equal and opposite to that produced by the gust, so that there is no net radiation from the edge [4].

The shedding does not become significant until Γ is close to the edge. It will be modelled by releasing from the edge A a succession of elementary line vortices of circulation Γ_k at discrete times $t = t_k$, $k \geq 1$. Let z_k, ζ_k denote respectively the position of Γ_k in the z-plane and its image in the upper half of the ζ-plane at time t. These vortices lie on the stagnation

streamline emanating from A (see Figure 6a), along which they convect at the local mean velocity; their images ζ_k are located on the line $\mathrm{Re}\,\zeta = 1$ extending from the real axis into the upper half-plane. At time t_j, when there are j shed vortices in the flow, the complex potential of the *unsteady* component of the flow is

$$w = \frac{-i\Gamma}{2\pi}\Big\{\ln(\zeta-\zeta_o) - \ln(\zeta-\zeta_o^*)\Big\} + \sum_{k=1}^{j}\frac{-i\Gamma_k}{2\pi}\Big\{\ln(\zeta-\zeta_k) - \ln(\zeta-\zeta_k^*)\Big\}. \qquad (60)$$

The Kutta condition is satisfied at A by setting $dw/d\zeta = 0$ at $\zeta = 1$. This determines the strength Γ_j of the jth vortex in terms of Γ and all of the previously shed vortices according to

$$\Gamma_j = -\mathrm{Im}\,\zeta_j\left\{\frac{\Gamma\,\mathrm{Im}\,\zeta_o}{|1-\zeta_o|^2} + \sum_{k=1}^{j-1}\frac{\Gamma_k}{\mathrm{Im}\,\zeta_k}\right\}. \qquad (61)$$

To apply this formula it is necessary to specify the initial position $\zeta_j = 1 + i\epsilon$ of the jth vortex on the stagnation streamline $\mathrm{Re}\,\zeta = 1$, where ϵ is small and positive, whose precise value does not materially affect the results. At the next time step in the calculation all of the shed vortices will have moved along this streamline by distances determined by the mean velocity potential (52).

The results of such a calculation are illustrated in Figure 6a, for the rounded airfoil considered previously. The initial stand-off distance d of Γ far upstream of the edge is equal to $\frac{1}{2}h$, as before, and the characteristic velocity u of (55) is again taken to be $-0.1U$. The trajectories of the incident and shed vortices are the streamlines of the mean flow shown in Figure 6a. Time is measured from the instant that Γ crosses $x_1 = 0$, and the figure shows the position of Γ at various times, and also the corresponding location of the peak shed vorticity. This peak is shed into the flow when Γ is close to the edge, and translates downstream with Γ on a parallel path at roughly the same velocity. Figure 6b indicates how the overall circulation of the wake vorticity is opposite in sign to Γ and has a final magnitude equal to about 80% of Γ. The slope of the wake circulation curve is always negative, showing that the sign of each elementary vortex Γ_j is always opposite to Γ.

The sound generated by the impinging vortex and the wake at the retarded time $t_j = t - |\mathbf{x}|/c_o$, just after the release of the jth vortex from A, can be calculated from either of the following generalizations of (58) and (59)

$$p'(\mathbf{x},t) \approx \frac{-\rho_o \sin(\theta/2)}{\pi^{\frac{3}{2}}}\sqrt{\frac{h}{|\mathbf{x}|}}\left(\frac{1+4\alpha/(1+\beta)^2}{1+\alpha}\right)^{\frac{1}{2}} \times \begin{cases} \mathrm{Im}\left[\Gamma\frac{d\zeta_o}{dt}+\sum_{k=1}^{j}\Gamma_k\frac{d\zeta_k}{dt}\right], \\ \\ \frac{1}{2\pi}\mathrm{Re}\left[\Gamma\frac{dz_o}{dt}\oint_S\frac{\zeta\,dz}{(z-z_o)^2}+\sum_{k=1}^{j}\Gamma_k\frac{dz_k}{dt}\oint_S\frac{\zeta\,dz}{(z-z_k)^2}\right], \end{cases} \quad |\mathbf{x}|\to\infty. \qquad (62)$$

The pressure signature is plotted against $U[t]/h$ in Figure 7. Also plotted are the separate contributions from Γ and from the wake, which are of comparable magnitudes, but opposite in sign. Because of the progressive increase in the total wake circulation, when $U[t]/h$ exceeds about 5 the separate acoustic pressures attributable to Γ and the wake are effectively equal an opposite. Thus, the net radiation is significantly different from zero only for retarded times $U[t]/h \sim \mathrm{O}(1)$ when Γ is very close to the sharp edge A. This may be contrasted with the analogous result for an airfoil of infinitesimal thickness [4], for which the predicted radiations from Γ and from the wake are equal an opposite for *all* times, and linear theory accordingly predicts that no sound is produced at the trailing edge.

5. CONCLUSION

In this chaapter the Chase-Chandiramani diffraction theory for estimating trailing edge noise from a flat plate, zero thickness airfoil has been extended to low Mach number flows past a non-compact airfoil of finite thickness and arbitrary trailing edge geometry. For the flat-plate, the radiation can be approximated by considering the diffraction at the edge of the boundary layer blocked pressure, which is assumed to convect in a frozen pattern past the edge. The same approximation for a thick airfoil significantly underpredicts the high frequency components of the sound. In this case the problem must be formulated in terms of the diffraction of the the boundary layer 'upwash' velocity. Both approaches are equivalent for the flat plate airfoil, but the extension permits account to be taken of modifications of the turbulence during convection past the variable geometry edge.

In applications it is desirable to be able to make accurate predictions of low Mach number edge noise by first performing numerical simulations of the edge flow based on the equations for an *incompressible* fluid, and then inserting the results into a suitable surface integral representation of the radiated sound. When the airfoil chord is not acoustically compact, it is *not* possible to make such predictions solely from a knowledge of the incompressible approximation to the unsteady surface pressure. This is because the airfoil itself extends into the acoustic far field, and the prescribed surface pressure must contain sufficient *acoustic* information to ensure that the calculated radiation satisfies the appropriate dynamical boundary conditions on the airfoil. In order to satisfy these conditions using incompressible data, the surface integral should involve an acoustic Green's function that is specifically tailored to the boundary conditions. For a rigid airfoil the normal derivative of the Green's function should vanish on its surface, and the incompressible data required to determine the far field sound is the boundary layer 'upwash' velocity. This velocity is equal to that given by the (free-field) Biot-Savart formula applied to the boundary layer vorticity lying *outside* the viscous sublayer.

REFERENCES

1. W. K. Blake and J. L. Gershfeld 1989 in *Lecture Notes in Engineering* 46 (Ed. M. Gad-el-Hak). Frontiers in Experimental Fluid Mechanics: The aeroacoustics of trailing edges.

2. T. F. Brooks, D. S. Pope and M. A. Marcolini 1989 *National Aeronautics and Space Administration Reference Publication No. 1218.* Airfoil self-noise and prediction.

3. D. G. Crighton 1991 Chapter 7 of *Aeroacoustics of Flight Vehicles: Theory and Practice* (Vol. 1). *National Aeronautics and Space Administration Reference Publication No. 1258.* Airframe noise.

4. M. S. Howe 1976 *Journal of Fluid Mechanics* **76**, 711 - 740. The influence of vortex shedding on the generation of sound by convected turbulence.

5. M. S. Howe. 1986 *Proceedings of the Royal Society* **A420**, 157 -182. Contributions to the theory of sound production by vortex-airfoil interaction, with application to vortices with finite axial velocity defect.

6. N. Curle 1955 *Proceedings of the Royal Society* **A231**, 505 -514. The influence of solid boundaries upon aerodynamic sound.

7. J. E. Ffowcs Williams and D. L. Hawkings 1969 *Philosophical Transactions of the Royal Society* **A264**, 321 -342. Sound generation by turbulence and surfaces in arbitrary motion.

8. M. J. Lighthill 1952 *Proceedings of the Royal Society* **A211**, 564 - 587. On sound generated aerodynamically. Part I: General theory.

9. M. J. Lighthill 1954 *Proceedings of the Royal Society* **A222**, 1 - 32. On sound generated aerodynamically. Part II: Turbulence as a source of sound.

10. J. E. Ffowcs Williams and L. H. Hall 1970 *Journal of Fluid Mechanics* **40**, 657 - 670. Aerodynamic sound generation by turbulent flow in the vicinity of a scattering half-plane.

11. D. M. Chase 1972 *Journal of the Acoustical Society of America* **52**, 1011 - 1023. Sound radiated by turbulent flow off a rigid hal-plane as obtained from a wavevector spectrum of hydrodynamic pressure.

12. K. L. Chandiramani 1974 *Journal of the Acoustical Society of America* **55**, 19 - 29. Diffraction of evanescent waves, with applications to aerodynamically scattered sound and radiation from unbaffled plates.

13. D. M. Chase 1975 *American Institute of Aeronautics and Astronautics Journal* **13**, 1041 - 1047. Noise radiated from an edge in turbulent flow.

14. R. K. Amiet 1976 *Journal of Sound and Vibration* **47**, 387 - 393. Noise due to turbulent flow past a trailing edge.

15. W. K. Blake 1986 *Mechanics of flow-induced sound and vibration*, Vol. 2: *Complex flow-structure interactions.* New York: Academic Press.

16. M. S. Howe 1978 *Journal of Sound and Vibration* **61**, 437 - 466. A review of the theory of trailing edge noise.

17. M. S. Howe 1998 *Reference manual on the theory of lifting surface noise at low Mach numbers.* Boston University, Department of Aerospace and Mechanical Engineering Report AM-98-001.

18. J. C. Hardin and J. E. Martin 1997 *American Institute of Aeronautics and Astronautics Journal* **35**, 810 - 815. Flap side-edge noise: acoustic analysis of Sen's model.

19. B. Noble 1958 *Methods based on the Wiener-Hopf Technique for the Solution of Partial Differential Equations.* Oxford: Pergamon Press. (Reprinted 1988, Chelsea Publishing Company, New York).

20. M. Abramowitz and I. A. Stegun (editors) 1970 *Handbook of Mathematical Functions* (ninth corrected printing), US Department of Commerce, National Bureau of Standards Applied Mathematics Series No.55.

21. M. S. Howe 1998 *Acoustics of Fluid-Structure Interactions*, Cambridge University Press.

22. D. M. Chase 1980 *Journal of Sound and Vibration* **70**, 29 - 67. Modeling the wavevector-frequency spectrum of turbulent boundary layer wall pressure.

23. G. M. Corcos 1964 *Journal of Fluid Mechanics* **18**, 353 - 378. The structure of the turbulent pressure field in boundary layer flows.

24. P. M. Morse and H. Feshbach 1953 *Methods of Theoretical Physics*, Vols. 1 and 2. New York: McGraw-Hill.

25. M. S. Howe 1975 *Journal of Fluid Mechanics* **71**, 625 - 673. Contributions to the theory of aerodynamic sound, with application to excess jet noise and the theory of the flute.

26. M. J. Lighthill 1958 *An introduction to Fourier analysis and generalised functions.* Cambridge University Press.

27. Horace Lamb 1932 *Hydrodynamics* (6th. ed.). Cambridge University Press (Reprinted 1993).

28. W. K. Blake 1983 in *Proceedings of the International Symposium on Turbulence Induced Vibrations and Noise of Structures*, (M. M. Sevik, editor). American Society of Mechanical Engineers, New York, pp 45 - 65. Excitation of plates and hydrofoils by trailing edge flows.

29. J. Gershfeld, W. K. Blake and C. W. Knisely 1988 *American Institute of Aeronautics and Astronautics Paper* 88-3826-CP Trailing edge flow and aerodynamic sound.

30. J. O. Hinze 1975 *Turbulence* (second edition). New York: McGraw-Hill.

31. G. K. Batchelor and I. Proudman 1954 *Quarterly Journal of Mechanics and Applied Mathematics* **7**, 83 - 103. The effect of rapid distortion of a fluid in turbulent motion.

32. H. S. Ribner and M. Tucker 1953 *National Advisory Committee on Aeronautics* Report No. 1113. Spectrum of turbulence in a contracting stream.

33. H. Ashley and M. Landahl 1965 *Aerodynamics of Wings and Bodies.* Reading MA: Addison-Wesley.

34. Y. C. Fung 1993 *An Introduction to the Theory of Aeroelasticity.* New York: Dover Publications Inc.

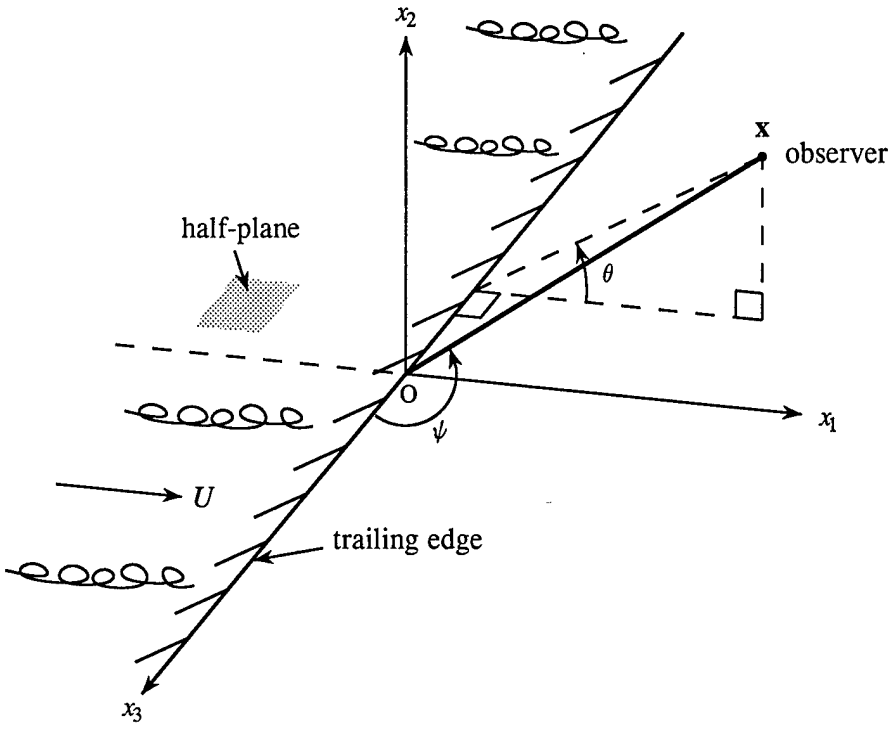

Figure 1. Coordinates for trailing edge noise.

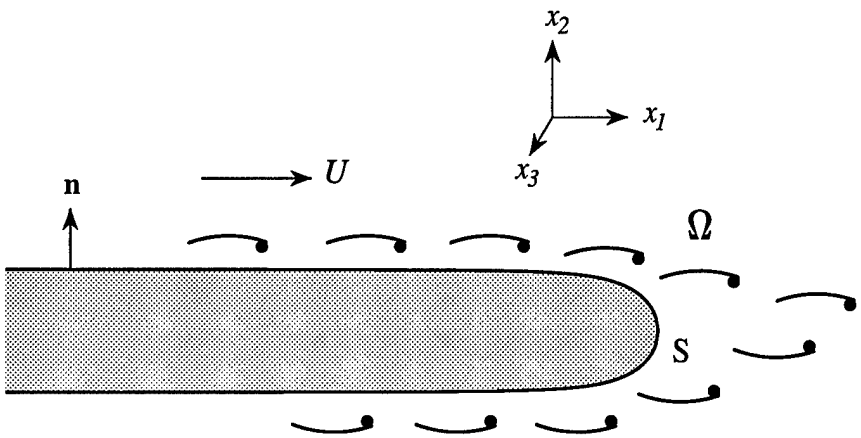

Figure 2. Low Mach number turbulent flow near the trailing edge of an airfoil of finite thickness.

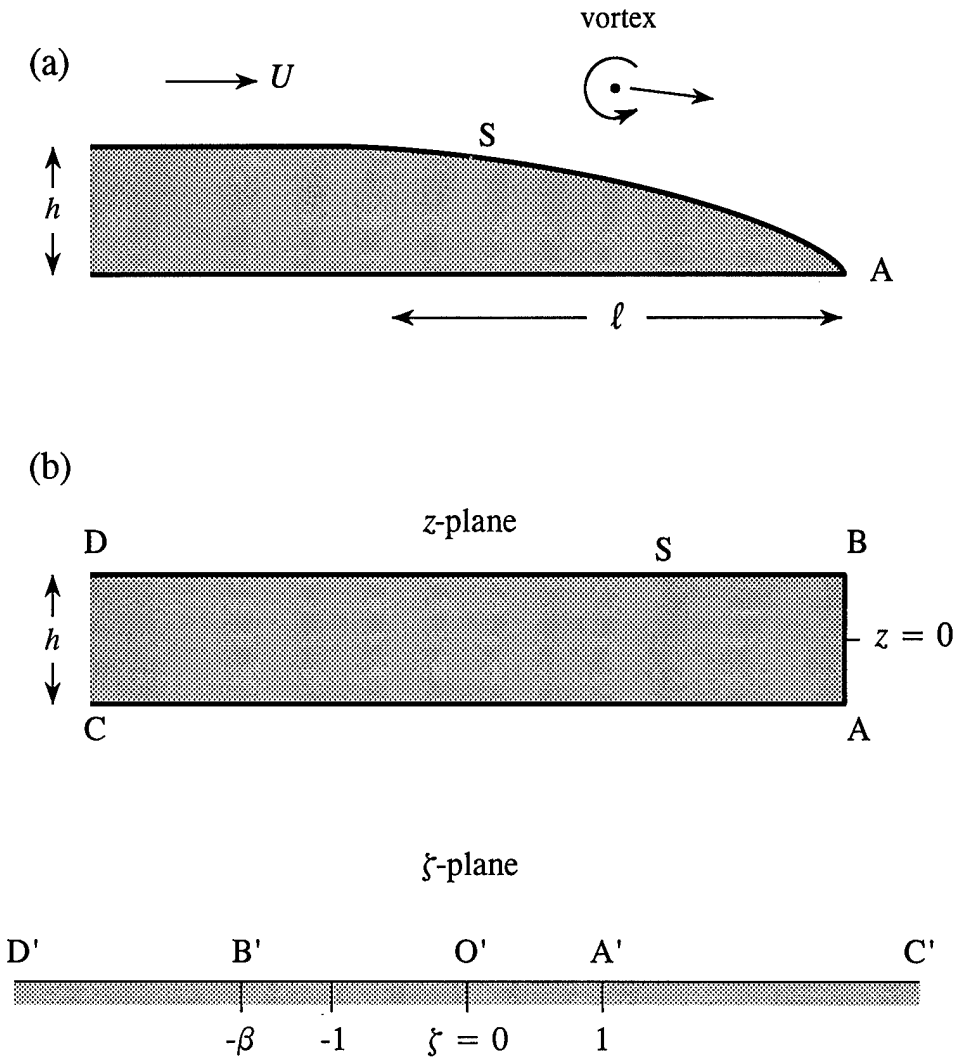

Figure 3. (a) Airfoil of thickness h with a rounded trailing edge section of length ℓ.
(b) Mapping the region outside a rectangular airfoil onto the upper half of the ζ-plane.

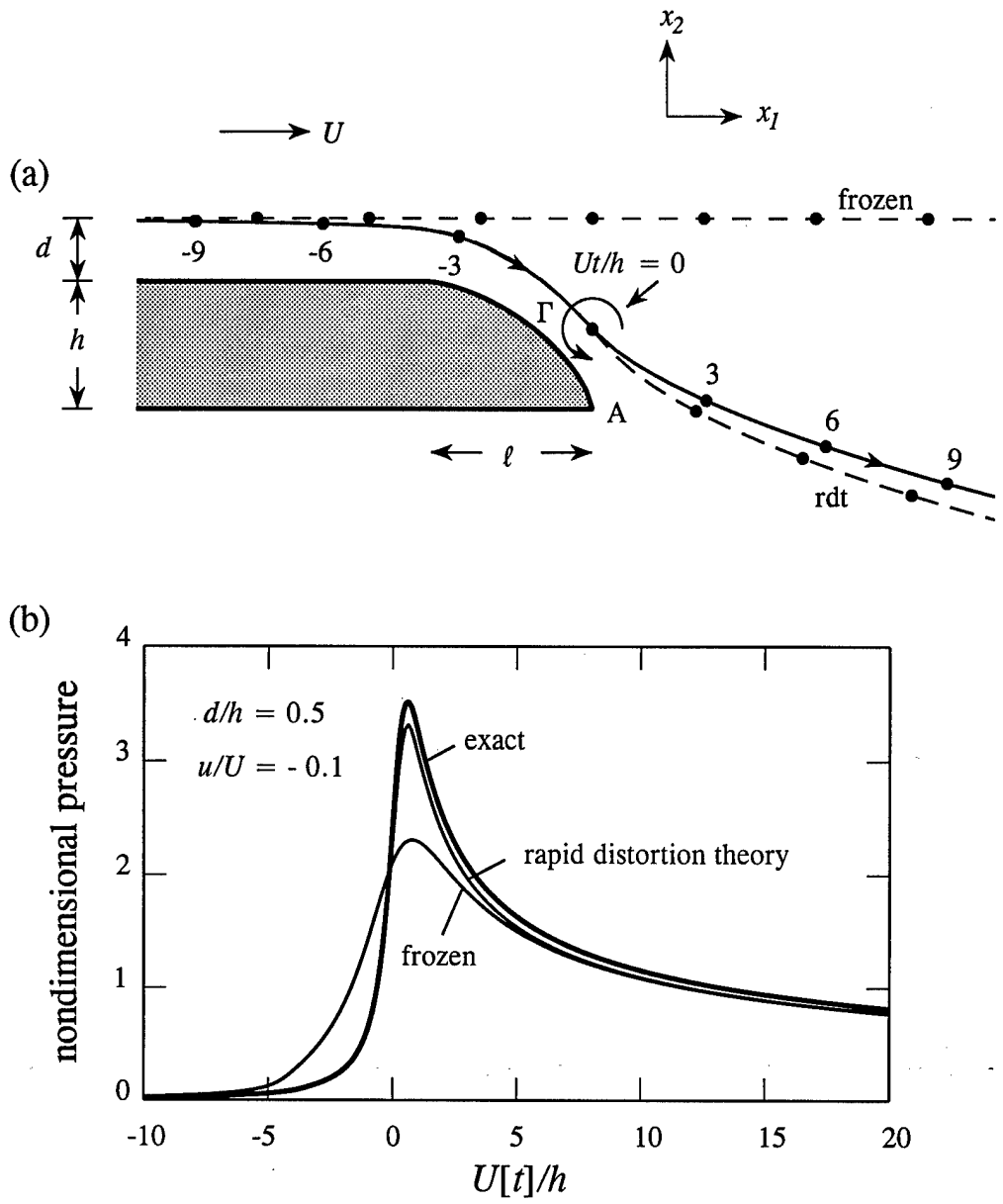

Figure 4. (a) Trajectories of the vortex Γ past the trailing edge when $u = -0.1U$, $\ell/h = 4$, $d/h = 0.5$. (b) Acoustic pressure signatures $p/\{\rho_o(\Gamma/h)^2 \sin(\theta/2)\sqrt{h/|\pi \mathbf{x}|}/8\}$.

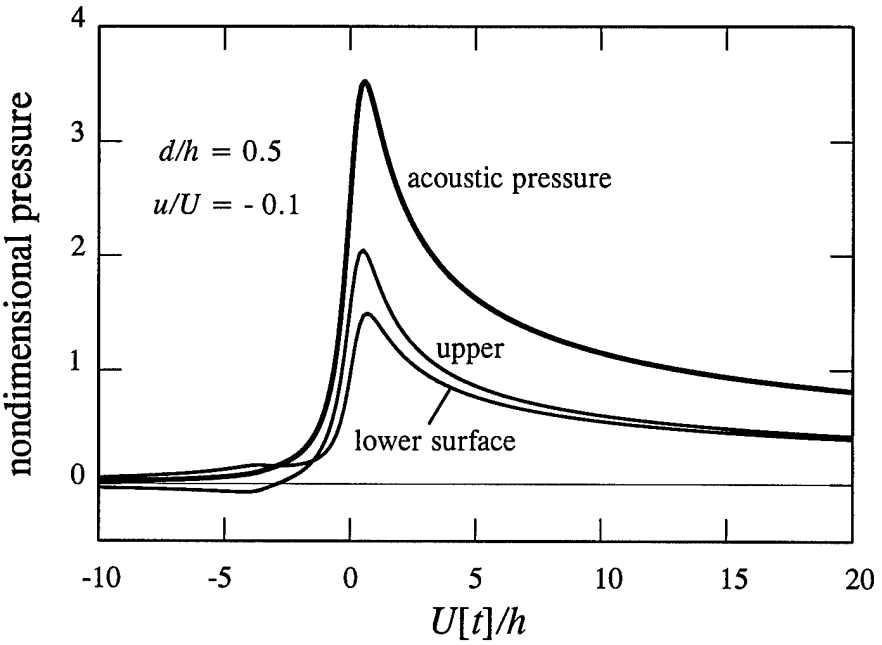

Figure 5. The acoustic pressure $p/\{\rho_o(\Gamma/h)^2 \sin(\theta/2)\sqrt{h/|\pi \mathbf{x}|}/8\}$ and the separate contributions from the upper and lower surfaces of the airfoil of Figure 4 when $u = -0.1U$, $\ell/h = 4$, $d/h = 0.5$ and when the vortex moves along the solid ('exact') trajectory of Figure 4a.

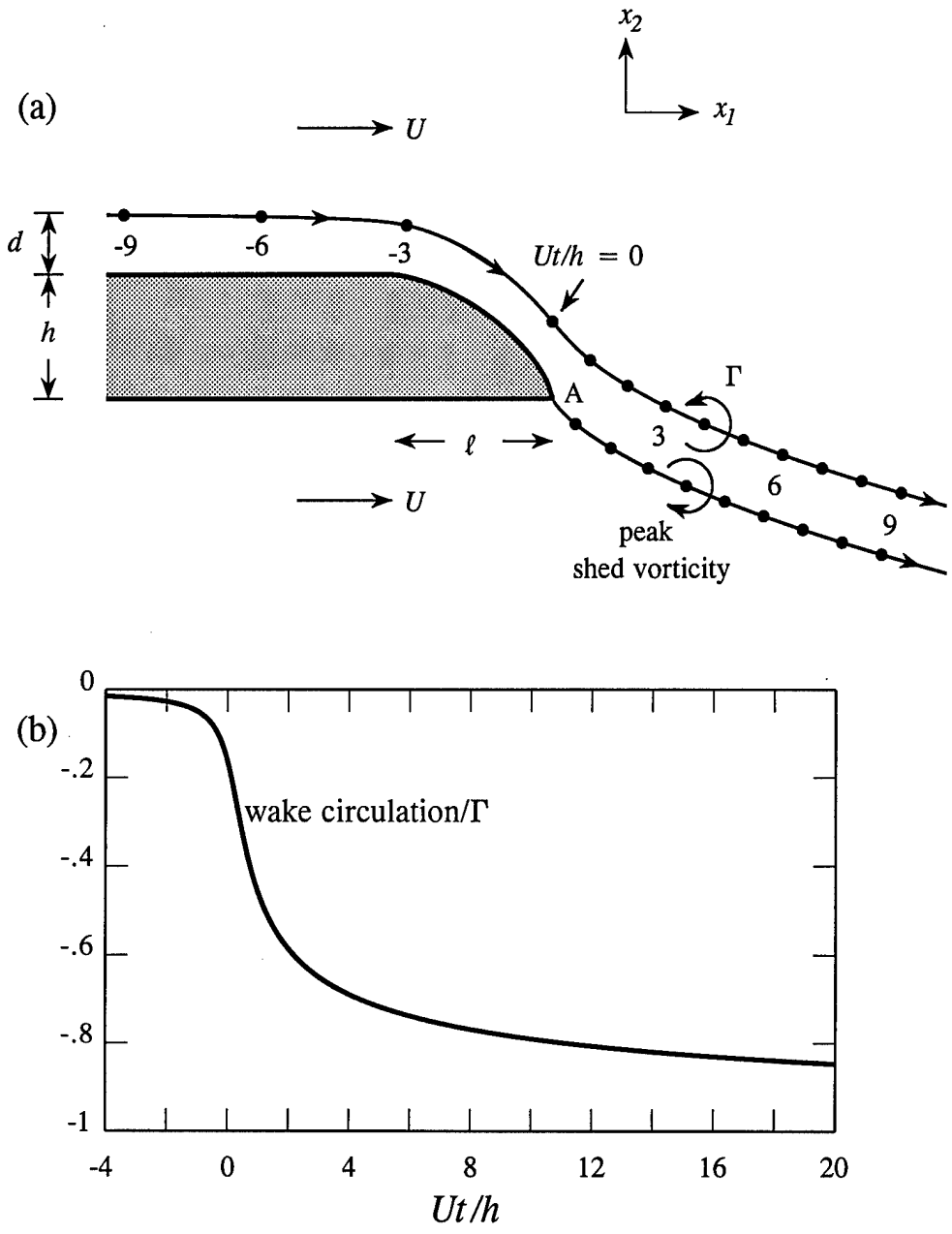

Figure 6. (a) Trajectories of the vortex Γ and shed vorticity in the approximation of rapid distortion theory for $u = -0.1U$, $\ell/h = 4$, $d/h = 0.5$
(b) Total wake circulation as a function of time.

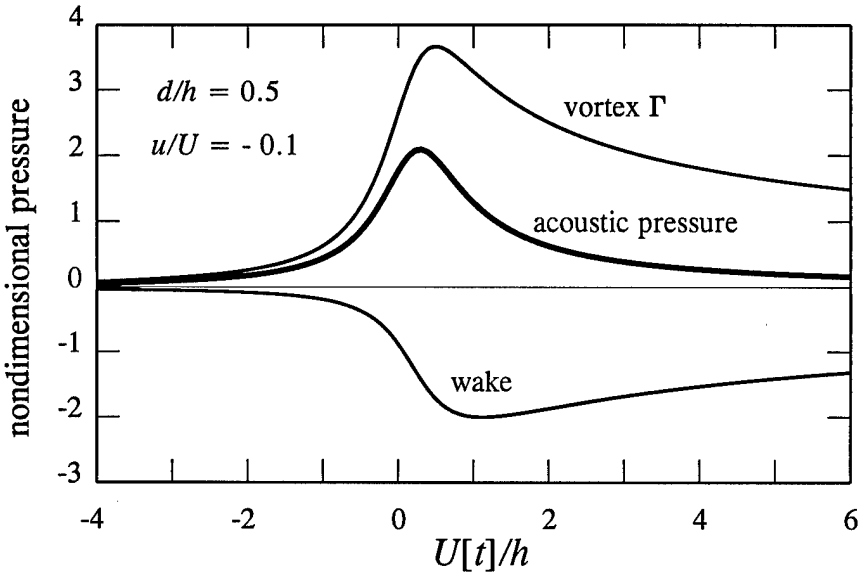

Figure 7. The acoustic pressure $p/\{\rho_o(\Gamma/h)^2 \sin(\theta/2)\sqrt{h/|\pi \mathbf{x}|}/8\}$ and the separate contributions from the vortex Γ and the vortex wake in the rapid distortion approximation of Figure 6, when $u = -0.1U$, $\ell/h = 4$, $d/h = 0.5$.

CHAPTER 2

ATTACHED AND SEPARATED EDGE FLOWS

SUMMARY

The diffraction theory of Chapter 1 is applied to investigate the noise produced by turbulent flow over an edge whose upper surface profile (the suction side) is rounded. The sound is expressed in terms of the 'upwash' velocity fluctuations that the same boundary layer turbulence would generate if the airfoil were absent. An approximate method is proposed for expressing these fluctuations in terms of local properties of the blocked pressure generated on the surface exposed to the turbulent flow. Predictions are made of the edge noise spectrum for both fully attached flow (that remains attached right up to the trailing edge) and for cases where separation occurs on the rounded profile. When premature separation occurs the amplitude of the edge-generated sound decreases exponentially with increasing frequency, and predicted edge noise levels are significantly smaller than estimates obtained when the airfoil is modeled by a rigid half plane. For attached flow turbulence on the suction side of the airfoil always passes close to the edge and interacts strongly with it, but contributions from the interaction of the same turbulence with the pressure side of the airfoil are reduced because of the finite airfoil thickness. In this case sound levels fall short of those for a rigid half plane typically by about 5 to 10 dB, the precise values being dependent on frequency, and on the ratio of the boundary layer thickness to the mean airfoil thickness.

1. INTRODUCTION

Consider turbulent flow at very small Mach number over the upper surface of the trailing edge an uncambered airfoil with a rounded upper surface edge profile, as illustrated in Figure 1. The profile is the same for all spanwise locations, so that the edge is parallel to the airfoil span. Airfoils of this type are frequently used in flow noise tests [1 - 3], and the simplified edge geometry is convenient for validating numerical codes for edge noise prediction. Let the main stream outside the airfoil boundary layers have low subsonic speed U in the x_1-direction of the rectangular coordinate axes (x_1, x_2, x_3). The coordinate origin O lies on the midplane of the airfoil in the 'vertical' plane of the trailing edge A (see Figure 2a, below). The upper, rounded edge region extends over the interval $-\ell < x_1 < 0$, and meets the lower surface at A: $x_1 = 0$, $x_2 = -\frac{1}{2}h$. Upstream of the edge, for $x_1 < -\ell$, the airfoil has uniform thickness h and its upper and lower surfaces coincide with the planes $x_2 = \pm\frac{1}{2}h$. The mean circulation around the airfoil is assumed to be adjusted to make A a stagnation point.

The theory of the self noise generated at a trailing edge of finite thickness is discussed in Chapter 1. When the airfoil thickness h is acoustically compact, it was shown that the acoustic pressure $p(\mathbf{x}, t)$ in the far at $\mathbf{x}$ at time t can be rendered in the form

$$p(\mathbf{x}, t) = \int_{-\infty}^{\infty} p(\mathbf{x}, \omega) \mathrm{e}^{-i\omega t}\, d\omega, \tag{1}$$

$$p(\mathbf{x}, \omega) \approx \frac{\rho_o \kappa_o^{\frac{1}{2}} \sin^{\frac{1}{2}}\psi \sin(\theta/2) \mathrm{e}^{i\kappa_o|\mathbf{x}|}}{\pi\sqrt{2\pi i}|\mathbf{x}|} \oint_S \left\{ i\omega\Phi^*(\mathbf{y}) v_{1n}(\mathbf{y}, \omega) + \nu\boldsymbol{\Omega}(\mathbf{y}, \omega) \wedge \frac{\partial\Phi^*(\mathbf{y})}{\partial \mathbf{y}} \cdot \mathbf{n} \right\} d\mathrm{S}(\mathbf{y}),$$
$$|\mathbf{x}| \to \infty, \tag{2}$$

where the integration is over the upper and lower surfaces S of the airfoil. The terms in this formula are defined as follows

$$\left.\begin{aligned} \rho_o &= \text{mean fluid density,} \\ \kappa_o &= \omega/c_o = \text{acoustic wavenumber,} \\ c_o &= \text{speed of sound,} \\ \nu &= \text{kinematic viscosity,} \\ \boldsymbol{\Omega} &= \text{curl } \mathbf{v} = \text{vorticity,} \quad \mathbf{v} = \text{velocity,} \\ \sin\psi &= r/|\mathbf{x}|, \quad r = \sqrt{x_1^2 + x_2^2}, \\ \sin\theta &= x_2/r. \end{aligned}\right\} \tag{3}$$

Thus, $(x_1, x_2) = r(\cos\theta, \sin\theta)$, and ψ is the angle between the radiation direction $\mathbf{x}/|\mathbf{x}|$ and the x_3-axis (the airfoil span, out of the plane of the paper in Figure 1).

$\Phi^*(\mathbf{x}) \equiv \Phi^*(x_1, x_2)$ is an auxiliary function that depends on the shape of the airfoil trailing edge profile. It satisfies Laplace's equation and describes an incompressible, irrotational flow around the edge of the airfoil (in planes parallel to the x_1x_2-plane), and is normalized such that

$$\Phi^*(x_1, x_2) \to \varphi^*(x_1, x_2) \equiv \sqrt{r}\sin(\theta/2), \quad \text{for } \sqrt{x_1^2 + x_2^2} \gg h, \tag{4}$$

where $\varphi^*(x_1, x_2)$ is the corresponding potential of irrotational flow (in the anticlockwise direction) about the edge of the *half plane* $x_1 < 0,\ x_2 = 0$.

The unit normal on S directed into the fluid is denoted by $\mathbf{n}$, and $v_{In} = \mathbf{v}_I \cdot \mathbf{n}$ is the normal component of the 'upwash velocity'. This is defined by

$$\frac{\partial \mathbf{v}_I}{\partial t} = -\text{curl} \int_V \frac{\text{curl}\,(\boldsymbol{\Omega} \wedge \mathbf{v}) d^3\mathbf{y}}{4\pi|\mathbf{x} - \mathbf{y}|} \equiv \text{curl} \int_V \left(\frac{\partial \boldsymbol{\Omega}}{\partial t} - \nu \nabla^2 \boldsymbol{\Omega} \right) \frac{d^3\mathbf{y}}{4\pi|\mathbf{x} - \mathbf{y}|}, \tag{5}$$

where V is the region occupied by the fluid. The vortical boundary layer motion is assumed to be well approximated at low Mach numbers by the Navier-Stokes equation for *incompressible* flow. In the viscous sublayer, close to the surface of the airfoil, the motion becomes *linear* and

$$\tfrac{\partial \boldsymbol{\Omega}}{\partial t} - \nu \nabla^2 \boldsymbol{\Omega} \approx \mathbf{0}.$$

Outside the sublayer viscous diffusion is negligible, and $\nu\nabla^2\boldsymbol{\Omega}$ may be discarded from the second integrand of (5). The upwash velocity is then given by the Biot-Savart formula [4]

$$\mathbf{v}_I(\mathbf{x}, t) = \text{curl} \int_{V_\delta} \frac{\boldsymbol{\Omega}(\mathbf{y}, t) d^3\mathbf{y}}{4\pi|\mathbf{x} - \mathbf{y}|}, \tag{6}$$

where the integration is confined to the nonlinear region of the boundary layer V_δ *outside* the viscous sublayer. This result implies that, in applications to flows of very large Reynolds numbers, where the dominant turbulent motions may be regarded as essentially inviscid, possible contributions to the integral (6) from *potential flow bound vorticity* on S must be excluded.

Equation (6) defines the velocity $\mathbf{v}_I$ in terms of the boundary layer vorticity *when the presence of the airfoil is ignored*, i.e., when the volume enclosed by S is imagined to contain fluid moving irrotationally at the induced velocity of the boundary layer vorticity. Of course, prior to evaluating the upwash velocity from either of the representations (5) or (6),

the vorticity $\boldsymbol{\Omega}(\mathbf{x}, t)$ and flow velocity $\mathbf{v}(\mathbf{x}, t)$ must first be determined with full account taken of the presence of the airfoil including, of course, the no-slip condition on S.

The first term in the brace brackets of the integrand of equation (2) represents the contribution to the edge noise from the *normal* surface stresses on S; the second term determines the net contribution from the surface shear stress, and is usually neglected at very high Reynolds numbers.

In Chapter 1 the two-dimensional version of equation (2) was used to examine the sound generated during the mean flow convection of a rectilinear vortex past the trailing edge of Figure 1, including the influence of vortex shedding induced from the edge A. In this chapter equation (2) will be applied to estimate the acoustic pressure frequency spectrum of the high frequency self noise generated by turbulent flow over the rounded edge profile. The theory is formulated (in §2) to enable account to be taken of changes in the mean turbulent boundary layer characteristics with distance from the edge. In the theory of edge noise generated by flow over the edge of a thin plate airfoil [5 - 7], the properties of the boundary layer turbulence are expressed in terms of the blocked wall pressure wavenumber-frequency spectrum, measured or specified empirically just upstream of the edge. In the present formulation (§3) it is assumed that the relevant frequencies are sufficiently high that the wavenumber-frequency spectrum of the *upwash velocity* v_{In} can be represented locally in terms of the blocked pressure spectrum, thereby permitting acoustic predictions to be made in terms of measured or calculated turbulence parameters. The Mach number is sufficiently small that the blocked pressure can be calculated from the incompressible equations of motion. Numerical results are presented in §3 for fully attached and separated edge flows, including a comparison with predictions of the *frozen* approximation of [5 - 7], according to which the boundary layer turbulence is convected over the edge along a path parallel to the undisturbed mean stream.

2. FORMAL REPRESENTATION OF THE EDGE NOISE

Introduce a curvilinear coordinate system $(s, s_\perp, x_3)$, where s is measured along the curvilinear stream lines of the potential function $\Phi^*(x_1, x_2)$ in the clockwise direction, $s_\perp$ lies in the x_1x_2-plane, normal to the streamlines and directed *away* from the profile S of the airfoil, on which we can take $s_\perp = 0$ (Figure 2a). Then, $s_\perp > 0$ in the fluid, and on S

$$v_{In} = \lim_{s_\perp \to -0} \frac{\partial \Phi}{\partial s_\perp}(s, s_\perp, x_3, \omega) \equiv \lim_{s_\perp \to -0} \frac{\partial}{\partial s_\perp} \int_{-\infty}^{\infty} \hat{\Phi}(s, s_\perp, k_3, \omega) e^{ik_3 x_3}\, dk_3, \tag{7}$$

where $\Phi(s, s_\perp, x_3, \omega)$, $\hat{\Phi}(s, s_\perp, k_3, \omega)$ are respectively the upwash velocity potential and its Fourier transform with respect to x_3. This potential is well defined throughout the whole of space where the vorticity $\boldsymbol{\Omega} = \mathbf{0}$, including the region occupied by the airfoil.

When the final representation in (7) is substituted for v_{In} in equation (2), with $d\mathrm{S} \equiv ds dy_3$, the integration with respect to y_3 yields the delta function $\delta(k_3)$. In an *exact* integral representation of the edge generated sound (involving the specification of *compressible* data on S) the surface integral would actually yield $\delta(k_3 - \kappa_0 \cos\psi)$, which merely implies that only those Fourier components of $v_{In}(s, x_3, \omega)$ that have supersonic spanwise phase velocity $|\omega/k_3| > c_0$ are responsible for the radiation of sound from the edge. In other words, the only relevant wavenumbers are confined to the *acoustic domain* $|k_3| < |\kappa_0|$, and correspond to variations in the spanwise direction occurring over distances of the order of the acoustic wavelength. However, the dominant hydrodynamic motions near the edge have length scales of the order of the boundary layer displacement thickness $\delta^* \ll 1/\kappa_0 < 1/|k_3|$. In the approximation of equation (2), $\kappa_0\delta^*$ is so small that we can take $k_3 \equiv 0$.

When $k_3 = 0$ and the source motion is regarded as incompressible, the velocity potential $\hat{\Phi}(s, s_\perp, k_3, \omega)$ satisfies Laplace's equation, which locally reduces to

$$\left(\frac{\partial^2}{\partial s^2} + \frac{\partial^2}{\partial s_\perp^2}\right) \hat{\Phi}(s, s_\perp, 0, \omega) = 0.$$

The corresponding *stream function* $\hat{\Psi}(s, s_\perp, \omega)$, say, is related to $\hat{\Phi}(s, s_\perp, 0, \omega)$ by the Cauchy-Riemann equations [4]

$$\frac{\partial \hat{\Psi}}{\partial s} = -\frac{\partial \hat{\Phi}}{\partial s_\perp}(s, s_\perp, 0, \omega), \quad \frac{\partial \hat{\Psi}}{\partial s_\perp} = \frac{\partial \hat{\Phi}}{\partial s}(s, s_\perp, 0, \omega). \tag{8}$$

Hence, substituting from (7) into equation (2), and discarding the contribution to the radiation from the surface shear stress, we find

$$p(\mathbf{x},\omega) \approx \frac{\rho_0\omega}{|\mathbf{x}|}\sqrt{\frac{2i\kappa_0}{\pi}}\sin^{\frac{1}{2}}\psi\sin(\theta/2)e^{i\kappa_0|\mathbf{x}|}\int_{-\infty}^{\infty}\Phi^*(\mathbf{y}(s))\left(\frac{\partial\hat{\Phi}}{\partial s_\perp}(s,s_\perp,0,\omega)\right)_{s_\perp=0}ds$$

$$= \frac{-\rho_0\omega}{|\mathbf{x}|}\sqrt{\frac{2i\kappa_0}{\pi}}\sin^{\frac{1}{2}}\psi\sin(\theta/2)e^{i\kappa_0|\mathbf{x}|}\int_{-\infty}^{\infty}\Phi^*(\mathbf{y}(s))\frac{\partial\hat{\Psi}}{\partial s}(s,0,\omega)\,ds, \quad |\mathbf{x}|\to\infty, \tag{9}$$

where the integration is taken in the clockwise sense around the profile $s_\perp = 0$ of the airfoil S.

Since the noise sources are confined to the neighborhood of the trailing edge, we may integrate by parts in the final line of (9) to express the radiation as a Stieltjes integral

$$p(\mathbf{x},\omega) \approx \frac{\rho_0\omega}{|\mathbf{x}|}\sqrt{\frac{2i\kappa_0}{\pi}}\sin^{\frac{1}{2}}\psi\sin(\theta/2)e^{i\kappa_0|\mathbf{x}|}\oint_S\hat{\Psi}(s,0,\omega)\,d\Phi^*, \quad |\mathbf{x}|\to\infty, \tag{10}$$

where the integration is in the clockwise direction about S. In §3 it will be convenient to evaluate the integral by setting $z = x_1 + ix_2$, and mapping the region of the z-plane outside the airfoil occupied by the fluid onto the upper half of the complex ζ-plane, such that the airfoil profile S transforms into the real ζ-axis with the correspondence of boundary points indicated in Figure 2b. But, the potential Φ^* is given in terms of ζ by

$$\Phi^* \equiv \Phi^*(z) = -\mu\mathrm{Re}\,\zeta, \quad \mu > 0, \tag{11}$$

where μ is a constant whose value depends on the shape of the trailing edge profile. Thus the acoustic pressure may be written

$$p(\mathbf{x},\omega) \approx -\frac{\rho_0\mu\omega}{|\mathbf{x}|}\sqrt{\frac{2i\kappa_0}{\pi}}\sin^{\frac{1}{2}}\psi\sin(\theta/2)e^{i\kappa_0|\mathbf{x}|}\int_{-\infty}^{\infty}\hat{\Psi}(s(\zeta),0,\omega)\,d\zeta, \quad |\mathbf{x}|\to\infty, \tag{12}$$

where the path of integration runs just above any singularities on the real axis.

3. MODELING HIGH FREQUENCY EDGE NOISE

3.1 Conformal mapping

The fluid region bounded internally by a trailing edge profile of the type shown in Figure 2a is mapped into the upper ζ-plane by means of the transformation

$$\frac{z}{h} = \frac{1}{(1+\alpha)}\Big[f(\zeta,1) + \alpha f(\zeta,\beta)\Big], \quad \alpha > 0, \quad \beta > +1, \tag{13}$$

where α and β are numerical constants, and

$$\begin{aligned} f(\zeta,\beta) \;=\; & -\frac{4}{\pi(1+\beta)^2}\left(\zeta + \frac{\beta-1}{2}\right)\sqrt{\zeta+\beta}\sqrt{\zeta-1} \\ & + \frac{1}{\pi}\ln\left[\left(\zeta + \frac{\beta-1}{2}\right) + \sqrt{\zeta+\beta}\sqrt{\zeta-1}\right] - \frac{i}{2} - \frac{1}{\pi}\ln\left(\frac{1+\beta}{2}\right). \end{aligned} \tag{14}$$

Equation (13) maps the real ζ-axis (Figure 2b) onto an airfoil profile S whose upper and lower surfaces coincide with $x_2 = \pm\frac{1}{2}h$ respectively for $\mathrm{Re}\,\zeta < -\beta$ and $\mathrm{Re}\,\zeta > 1$. This transformation divides the upper, rounded section of the trailing edge (between B and A in Figure 2a) in two sections: the interval $-\beta < \mathrm{Re}\,\zeta < -1$ is the image of the section that starts at B and terminates (at $\zeta = -1$) at the top of a vertical 'end-face' ($x_1 = 0$, $-\frac{1}{2}h < x_2 < -\frac{1}{2}h + \Delta$) of thickness Δ, which corresponds to the interval $-1 < \mathrm{Re}\,\zeta < 1$. The values of α and β are calculated by prescribing values for the geometrical ratios ℓ/h and Δ/h. As in Chapter 1, results presented in this chapter are for

$$\alpha = 600, \quad \beta = 86.9370 \tag{15}$$

which yield $\ell/h = 4$ and $\Delta/h = 0.0074$. The corresponding airfoil profile is shown in Figure 2a (because $\Delta \ll h$ the end-face cannot be distinguished).

The coefficient μ in the definition (11) of Φ^* is determined from condition (4), which is equivalent to $-\mu\zeta \to -i\sqrt{z}$ as $|z|/h \to \infty$, and supplies

$$\mu = \sqrt{\frac{h}{\pi(1+\alpha)}\left(1 + \frac{4\alpha}{(1+\beta)^2}\right)}. \tag{16}$$

3.2 The frozen approximation

In the *frozen approximation* of thin airfoil theory [5 - 7] the boundary layer turbulence is assumed to convect parallel to the undisturbed mean stream at a convection velocity U_c,

which depends weakly on frequency ω. When this is applied to the airfoil of Figure 2a, boundary layer eddies translate as frozen distributions of vorticity in the x_1-direction within a boundary layer constrained to lie above the plate in the $x_2 > \frac{1}{2}h$, so that the separation streamline is parallel to the undisturbed mean flow velocity, and extends downstream parallel to the x_1 axis. $\hat{\Psi}$ satisfies Laplace'e equation in the region $x_2 \leq \frac{1}{2}h$, where we can write

$$\hat{\Psi}(x_1, x_2, \omega) = \int_{-\infty}^{\infty} \mathcal{A}(k,\omega) \mathrm{e}^{ikx_1 - |k|(h/2 - x_2)}\, dk, \qquad x_2 \leq \frac{1}{2}h. \tag{17}$$

It was shown in Chapter 1 (§3.2) that the pressure fluctuations $p_{\mathrm{I}}(\mathbf{x}, t)$ produced by the boundary layer turbulence in $x_2 \leq \frac{1}{2}h$ *when the presence of the airfoil is ignored* satisfies the linear relation $\partial \mathbf{v}_{\mathrm{I}}/\partial t = (-1/\rho_{\mathrm{o}})\nabla p_{\mathrm{I}}$, and it therefore follows by applying this relation on $x_2 = \frac{1}{2}h$ that

$$\mathcal{A}(k,\omega) = \frac{\mathrm{sgn}(k)}{2\rho_{\mathrm{o}}\omega}\, p_s(k, 0, \omega), \tag{18}$$

$p_s(k, k_3, \omega)$ being the Fourier transform of the blocked wall pressure, defined by

$$p_s(k, k_3, \omega) = \frac{1}{(2\pi)^3} \int_{-\infty}^{\infty} p_s(x_1, x_3, t) \mathrm{e}^{-i\{kx_1 + k_3 x_3 - \omega t\}}\, dx_1 dx_3 dt, \tag{19}$$

where $p_s(x_1, x_3, t) \equiv 2p_{\mathrm{I}}(x_1, h/2, x_3, t)$ is the pressure that would be exerted by the boundary layer on a rigid wall at $x_2 = \frac{1}{2}h$, i.e., on the upstream, flat section of the upper surface of the airfoil. In the frozen approximation it is assumed that measurements of $p_s(x_1, x_3, t)$ several characteristic hydrodynamic length scales upstream of the trailing edge are sufficient to determine $p_s(k, k_3, \omega)$.

Then, in equation (12) we find

$$\int_{-\infty}^{\infty} \hat{\Psi}(s(\zeta), 0, \omega)\, d\zeta \;=\; \frac{1}{2\rho_{\mathrm{o}}\omega} \int_{-\infty}^{\infty} \mathcal{I}(k) p_s(k, 0, \omega)\, dk, \tag{20}$$

$$\mathcal{I}(k) \;=\; \begin{cases} \text{c.c.} \left\{ \mathrm{e}^{-kh/2} \int_{-\infty}^{\infty} \mathrm{e}^{-ikz}\, d\zeta \right\} & \text{for } \; k > 0, \\ -\text{c.c.}\{\mathcal{I}(-k)\} & \text{for } \; k < 0, \end{cases} \tag{21}$$

where 'c.c.' denotes the complex conjugate. Thus, equations (12) and (1) give the far field sound in the form

$$p(\mathbf{x}, t) \approx -\frac{\mu \sin^{\frac{1}{2}} \psi \sin(\theta/2)}{\sqrt{2\pi c_{\mathrm{o}}}|\mathbf{x}|} \iint_{-\infty}^{\infty} \omega^{\frac{1}{2}} \mathcal{I}(k) p_s(k, 0, \omega) \mathrm{e}^{-i\omega(t - |\mathbf{x}|/c_{\mathrm{o}}) + \frac{i\pi}{4}}\, dk d\omega, \quad |\mathbf{x}| \to \infty. \tag{22}$$

The acoustic pressure frequency spectrum $\Phi(\mathbf{x}, \omega)$, which satisfies

$$\langle p^2(\mathbf{x}, t) \rangle = \textstyle\int_0^{\infty} \Phi(\mathbf{x}, \omega) d\omega,$$

the angle brackets $\langle\ \rangle$ denoting an ensemble average, is calculated from (22) by first assuming that only a finite spanwise section $-\frac{1}{2}L < x_3 < \frac{1}{2}L$ of the trailing edge is wetted by the turbulent flow, where L is much larger than the boundary layer thickness δ. For statistically stationary turbulence

$$\langle p_s(k,0,\omega)p_s^*(k',0,\omega')\rangle \approx \frac{L}{2\pi}\delta(\omega-\omega')\delta(k-k')\mathrm{P}(k,0,\omega), \quad L \gg \delta, \tag{23}$$

where the asterisk represents the complex conjugate, and $\mathrm{P}(k,k_3,\omega) \equiv \mathrm{P}(-k,k_3,-\omega)$ is the wavenumber-frequency spectrum of the blocked wall pressure [8]. Then equation (22) yields

$$\Phi(\mathbf{x},\omega) = \frac{\mu^2 \sin\psi \sin^2(\theta/2)}{2\pi^2|\mathbf{x}|^2}\frac{\omega L}{c_o}\int_{-\infty}^{\infty}|\mathcal{I}(k)|^2\mathrm{P}(k,0,\omega)\,dk, \quad |\mathbf{x}| \to \infty. \tag{24}$$

To illustrate predictions of this formula the wall pressure spectrum will be approximated by the Corcos formula, which is applicable for $\omega\delta/U > 1$ in the immediate neighborhood of the 'convective ridge' (where $\mathrm{P}(k,k_3,\omega)$ attains a large maximum) [9]:

$$\begin{aligned}\mathrm{P}(k,k_3,\omega) &= \Phi_{pp}(\omega)\frac{\ell_1}{\pi[1+\ell_1^2(k-\omega/U_c)^2]}\frac{\ell_3}{\pi[1+\ell_3^2k_3^2]} \\ \ell_1 &\approx 9U_c/\omega, \quad \ell_3 \approx 1.4U_c/\omega.\end{aligned} \tag{25}$$

The lengths ℓ_1 and ℓ_3 are frequency dependent turbulence correlation scales in the x_1- and x_3-directions. Φ_{pp} is the *point pressure frequency spectrum* which will be approximated by the following empirical formula (based on data collated by Chase [8]):

$$\frac{(U/\delta_*)\Phi_{pp}(\omega)}{(\rho_o v_*^2)^2} = \frac{(\omega\delta_*/U)^2}{[(\omega\delta_*/U)^2+\alpha_p^2]^{\frac{3}{2}}}, \quad \alpha_p = 0.12, \tag{26}$$

where $\delta_* \sim \delta/8$ is the boundary layer displacement thickness, and v_* is the friction velocity.

The principal contribution to the integral in (24) is from the immediate vicinity of the spectral maximum in the convective ridge, where $k \sim \omega/U_c$. We therefore replace $\mathcal{I}(k)$ by $\mathcal{I}(\omega/U_c)$ to obtain

$$\begin{aligned}\Phi(\mathbf{x},\omega) &\approx \frac{\mu^2 \sin\psi \sin^2(\theta/2)}{2\pi^2|\mathbf{x}|^2}\frac{\omega L}{c_o}\left|\mathcal{I}\left(\frac{\omega}{U_c}\right)\right|^2\int_{-\infty}^{\infty}\mathrm{P}(k,0,\omega)\,dk \\ &\approx \frac{0.7LM_c\mu^2 \sin\psi \sin^2(\theta/2)}{\pi^3|\mathbf{x}|^2}\left|\mathcal{I}\left(\frac{\omega}{U_c}\right)\right|^2\Phi_{pp}(\omega), \quad |\mathbf{x}| \to \infty,\end{aligned} \tag{27}$$

where the $M_c = U_c/c_o$ is the convection Mach number.

The integral in (21) defining $\mathcal{I}(k)$ must be evaluated numerically, with $z = z(\zeta)$ determined by equation (13). Then the acoustic frequency spectrum can be expressed in the nondimensional form

$$\frac{(U/\delta_*)\Phi(\mathbf{x},\omega)}{(\rho_o v_*^2)^2} \approx \mu^2 M \left(\frac{L\delta_*}{|\mathbf{x}|^2}\right) \sin\psi \sin^2\left(\frac{\theta}{2}\right) \left(\frac{\omega}{\pi U_c}\right) \left|\mathcal{I}\left(\frac{\omega}{U_c}\right)\right|^2 \frac{a_o(\omega\delta_*/U)}{[\alpha_p^2 + (\omega\delta_*/U)^2]^{\frac{3}{2}}}, \quad a_0 = 0.035, \tag{28}$$

where $M = U/c_o$ is the Mach number of the main stream, and we have introduced the approximation $U_c \approx 0.7U$; μ is given by (16).

The solid curve in Figure 3 is a nondimensional plot of the acoustic pressure spectrum for the particular case $h = \delta$, when the thickness of the turbulent boundary layer over the upper surface is just equal to the airfoil thickness h. At very low frequencies (when $\omega h/U_c \ll 1$) the radiation must be similar to that from the edge of a thin rigid half-plane. In this limit

$$\mathcal{I}\left(\frac{\omega}{U_c}\right) \sim \frac{e^{-\frac{i\pi}{4}}}{\mu}\sqrt{\frac{\pi U_c}{\omega + i0}}, \quad \frac{\omega h}{U_c} \ll 1, \tag{29}$$

and the spectrum becomes identical with that for the half plane

$$\frac{(U/\delta_*)\Phi(\mathbf{x},\omega)}{(\rho_o v_*^2)^2} \approx M \left(\frac{L\delta_*}{|\mathbf{x}|^2}\right) \sin\psi \sin^2\left(\frac{\theta}{2}\right) \frac{a_o(\omega\delta_*/U)}{[\alpha_p^2 + (\omega\delta_*/U)^2]^{\frac{3}{2}}}, \tag{30}$$

which is also plotted in Figure 3.

The large difference at high frequencies between the half plane and rounded edge spectra occurs because, in the frozen approximation the perpendicular stand-off distance of the separation streamline from the edge A (where the high frequency noise is generated) is equal to the plate thickness h, so that the upwash velocity at the edge is reduced by a factor of order $e^{-|\omega|h/U_c} \ll 1$ relative to the half plane.

3.3 Fully attached edge flow

When the turbulent boundary layer remains attached to the curved upper surface of the airfoil right up to the edge A, as indicated in Figure 4, we write the representation (17) for $\hat{\Psi}(x_1, x_2, \omega)$ on the *upper* surface in terms of $(s, s_\perp)$ in the form

$$\hat{\Psi}(s, s_\perp, \omega) = \int_{-\infty}^{\infty} \mathcal{A}(k,\omega) e^{iks - |k|s_\perp}\, dk, \quad s_\perp \le 0, \quad \zeta < 1. \tag{31}$$

$\mathcal{A}(k,\omega)$ is determined by assuming that the wall pressure Fourier transform $p_s(k, 0, \omega)$ is defined *locally* on the curved surface, with local statistical properties defined as in (23) - (26) that may vary over length scales much larger than the correlation scale of the turbulence.

This approximation can be used to evaluate the portion $\int_{-\infty}^{1} \hat{\Psi}(s(\zeta),0,\omega)\,d\zeta$ of the integral in the representation (12) of the sound pressure. On the lower surface of the airfoil (i.e., for $1<\zeta<+\infty$), we apply a local plane wave approximation to (31) by writing

$$\hat{\Psi}(s,0,\omega)=\int_{-\infty}^{\infty}\mathcal{A}(k,\omega)\mathrm{e}^{ik\{s'(\zeta)+h'(\zeta)\sin\vartheta\}-|k|h'(\zeta)\cos\vartheta}\,dk,\qquad s_\perp=0,\quad \zeta>1, \tag{32}$$

where for a point on the lower surface specified by ζ $(1<\zeta<+\infty)$ $s'(\zeta)$ is the value of s at the *corresponding point on the upper surface* (i.e., where the perpendicular from the lower surface point meets the upper surface), $h'(\zeta)$ is the airfoil thickness at that point, and $\vartheta=\vartheta(\zeta)$ is the angle between the $s_\perp$-axis and the x_2-direction at the upper surface point. Thus, when $\mathcal{A}(k,\omega)$ is approximated in terms of the blocked pressure as in (18), the far field sound is found to be given by

$$\begin{aligned} p(\mathbf{x},t) \;\approx\; & \frac{-\mu\sin^{\frac{1}{2}}\psi\sin(\theta/2)}{|\mathbf{x}|\sqrt{2\pi c_0}}\iint_{-\infty}^{\infty}dkd\omega\int_{-\infty}^{1}\mathrm{sgn}(k)\sqrt{i\omega}p_s(k,0,\omega)\mathrm{e}^{iks(\zeta)} \\ & \times\left[1+\left(\frac{d\bar{\zeta}}{d\zeta}\right)\mathrm{e}^{ikh'(\bar{\zeta})\sin\bar{\vartheta}-|k|h'(\bar{\zeta})\cos\bar{\vartheta}}\right]\mathrm{e}^{-i\omega(t-|\mathbf{x}|/c_0)}\,d\zeta \end{aligned} \tag{33}$$

where, for $-\infty<\zeta<1$, $\bar{\zeta}(\zeta)$ is determined by the point of intersection with the lower surface of the perpendicular onto the latter from the point ζ on the upper surface, so that $1<\bar{\zeta}<+\infty$, and $\bar{\vartheta}=\vartheta(\bar{\zeta})$.

Thus, forming the acoustic pressure frequency spectrum, as in §3.2, we obtain the following modified form of equation (24)

$$\begin{aligned} \Phi(\mathbf{x},\omega) \;\approx\; & \frac{\mu^2\sin\psi\sin^2(\theta/2)}{2\pi^2|\mathbf{x}|^2}\frac{\omega L}{c_0}\int_{-\infty}^{\infty}dk\iint_{-\infty}^{1}\mathrm{P}(k,0,\omega)\mathrm{e}^{ik\{s(\zeta)-s(\zeta')\}} \\ & \times\left[1+\left(\frac{d\bar{\zeta}}{d\zeta}\right)\mathrm{e}^{ikh'(\bar{\zeta})\sin\bar{\vartheta}-|k|h'(\bar{\zeta})\cos\bar{\vartheta}}\right]\left[1+\left(\frac{d\bar{\zeta}'}{d\zeta'}\right)\mathrm{e}^{-ikh'(\bar{\zeta}')\sin\bar{\vartheta}'-|k|h'(\bar{\zeta}')\cos\bar{\vartheta}'}\right]d\zeta d\zeta', \\ & |\mathbf{x}|\to\infty. \end{aligned} \tag{34}$$

We can take account of slow changes (on a scale of the boundary layer thickness δ) in the mean properties of the boundary layer turbulence with curvilinear distance along the airfoil by permitting $\mathrm{P}(k,0,\omega)$ in (34) to be a slowly varying function of $s=s(\zeta)$ and $s'=s(\zeta')$. The simplest way to do this is to use a modified form of the Corcos approximation (25) in which the point pressure frequency spectrum $\Phi_{pp}(\omega)$ is replaced by the geometric mean $\sqrt{\Phi_{pp}(s,\omega)\Phi_{pp}(s',\omega)}$ of the corresponding spectra at s and s', *viz.*

$$\mathrm{P}(k,k_3,\omega)=\sqrt{\Phi_{pp}(s,\omega)\Phi_{pp}(s',\omega)}\frac{\ell_1}{\pi[1+\ell_1^2(k-\omega/U_c)^2]}\frac{\ell_3}{\pi[1+\ell_3^2k_3^2]}. \tag{35}$$

This would be appropriate if variations in the convection velocity $U_c \approx 0.7U$ are small compared with changes in the structure of the point pressure spectrum Φ_{pp} as the trailing edge is approached. It is necessary to take the geometric mean (as opposed to, say, the arithmetic mean) to ensure that the right hand side of (34) remains positive definite.

Thus, when the wavenumber integral in (34) is evaluated as before, by taking the first term in the expansion about the convective peak at $k = \omega/U_c$, we find

$$\Phi(\mathbf{x},\omega) \approx \frac{0.7\mu^2 LM \sin\psi \sin^2(\theta/2)}{\pi^3|\mathbf{x}|^2}|\mathcal{F}(\omega)|^2, \quad |\mathbf{x}| \to \infty,$$

$$\mathcal{F}(\omega) = \int_{-\infty}^{1} \sqrt{\Phi_{pp}(s,\omega)}\left[1 + \left(\frac{d\bar{\zeta}}{d\zeta}\right) \mathrm{e}^{ikh'(\bar{\zeta})\sin\bar{\vartheta} - |k|h'(\bar{\zeta})\cos\bar{\vartheta}}\right] \mathrm{e}^{iks(\zeta)}\, d\zeta. \tag{36}$$

In the numerical results to be given below we shall ignore the dependence of $\Phi_{pp}(s,\omega)$ on s. In that case the acoustic pressure spectrum has the form given previously in equation (28), with

$$\mathcal{I}(k) = \mathrm{sgn}(k) \int_{-\infty}^{1} \left[1 + \left(\frac{d\bar{\zeta}}{d\zeta}\right) \mathrm{e}^{ikh'(\bar{\zeta})\sin\bar{\vartheta} - |k|h'(\bar{\zeta})\cos\bar{\vartheta}}\right] \mathrm{e}^{iks(\zeta)}\, d\zeta. \tag{37}$$

This integral must be evaluated numerically. In doing this it has been assumed that the separation streamline at the edge makes an angle $-\frac{\pi}{4}$ with the positive direction of the x_1-axis, which is the same as for potential flow past the airfoil when the Kutta condition is applied at A (see Chapter 1). In order to achieve this smooth behavior, we have set $\bar{\vartheta} = \frac{\pi}{4}$ at those points very close to A where the geometrical value of the angle actually exceeds $\frac{\pi}{4}$.

The acoustic pressure frequency spectrum is given by equation (28). It is plotted in Figure 4 for $h/\delta = 1$ and 5. The intensity of the sound decreases as h/δ increases, because the exponential decay of the second term in the square brackets of (37) rapidly reduces the contribution from the lower surface. However, the full effect of scattering by the upper surface is always present, so that the overall reductions with increasing thickness are very much less than those predicted by the frozen approximation.

3.4 Separated edge flow

When the boundary layer separates at some intermediate point on the curved section of the trailing edge (Figure 5) the radiation can be estimated by combining the approximations of §§3.2, 3.3. Let separation occur at $x_1 = x_0$ ($\zeta = \zeta_0$), at the point where the airfoil

thickness is h_o, and assume that immediately after separation the turbulence convects in a frozen pattern parallel to the undisturbed mean stream. In the simplest approximation in which the dependence of $\Phi_{pp}(s,\omega)$ on s is again ignored, the acoustic pressure spectrum can be set in the form (28), where

$$\mathcal{I}(k) = \mathrm{sgn}(k)\Bigg\{\int_{-\infty}^{\zeta_o}\left[1+\left(\frac{d\bar{\zeta}}{d\zeta}\right)e^{ikh'(\bar{\zeta})\sin\bar{\vartheta}-|k|h'(\bar{\zeta})\cos\bar{\vartheta}}\right]e^{iks(\zeta)}\,d\zeta + \int_{\zeta_o}^{1}\left[e^{-|k|d(\zeta)}+\left(\frac{d\bar{\zeta}}{d\zeta}\right)e^{-|k|h_o}\right]e^{ik(s_o+x_1-x_o)}\,d\zeta\Bigg\}, \quad (38)$$

where $d(\zeta) = h_o - \frac{1}{2}h - x_2(\zeta)$ $(\zeta < 1)$ is the vertical standoff distance of the separation streamline from the upper surface of the airfoil, and $s_o = s(\zeta_o)$. The separation coordinate x_o and the curvilinear distance of the separation point from the edge are displayed in Table 1.

h_o/h	x_o/h	curvilinear distance/h
1	-4	4.19
0.5	-0.97	1.11
0.2	-0.24	0.32
0.1	-0.08	0.13

Table 1. Separation coordinates for $\alpha = 600$, $\beta = 86.9370$.

Typical acoustic pressure frequency spectra, calculated from the general formula (28), are illustrated in Figure 5 for the cases of Table 1 when $\delta = h$. The contributions at high frequencies decay very rapidly as the separation point moves upstream from the edge, for the reasons discussed in §3.2. The case $h_o/h = 1$ coincides with the frozen approximation of §3.2.

These results (and the frozen approximation of §3.2) take no account of the sound generated by turbulence in the 'dead water' region bounded by the separation streamline and the curved section of the upper surface between the separation point and the edge.

4. CONCLUSION

The intensity of the high frequency sound generated by turbulent flow past the trailing edge of an airfoil is significantly reduced if separation occurs upstream of the geometrical edge. Separated flow over a curved trailing edge profile (Figure 5) can be modeled by assuming that after separation boundary layer eddies are convected along a path parallel to the undisturbed mean stream, so that their distance of closest approach to the sharp trailing edge is just equal to the airfoil thickness at the separation point. The strength of the unsteady interaction responsible for sound generation then decreases exponentially with increasing frequency, and predicted levels of edge noise are significantly smaller than estimates made by modelling the interaction in terms of a rigid half plane. This conclusion ignores possible contributions to sound generation from turbulence in the recirculating zone between the separation streamline and the curved section of the upper surface between the separation point and the edge, which are probably significant only at much lower frequencies [1].

When the mean flow remains attached right up to the trailing edge, boundary layer turbulence on the suction side of the airfoil always interacts strongly with the edge. However, because of the finite thickness of the airfoil, the influence of the (turbulence free) lower surface on the radiated intensity continues to decrease exponentially fast at high frequencies. In consequence, most of the high frequency radiation is associated with the flow interacting with the upper surface. The sound levels are smaller than for the half plane model, but the differences at higher frequencies are more modest, typically being of the order 5 to 10 dB, the precise values being dependent on the ratio of the boundary layer thickness to the mean airfoil thickness.

REFERENCES

1. W. K. Blake and J. L. Gershfeld 1989 in *Lecture Notes in Engineering* 46 (Ed. M. Gad-el-Hak). Frontiers in Experimental Fluid Mechanics: The aeroacoustics of trailing edges.

2. W. K. Blake 1983 in *Proceedings of the International Symposium on Turbulence Induced Vibrations and Noise of Structures*, (M. M. Sevik, editor). American Society of Mechanical Engineers, New York, pp 45 - 65. Excitation of plates and hydrofoils by trailing edge flows.

3. J. Gershfeld, W. K. Blake and C. W. Knisely 1988 *American Institute of Aeronautics and Astronautics Paper* 88-3826-CP Trailing edge flow and aerodynamic sound.

4. Horace Lamb 1932 *Hydrodynamics* (6th. ed.). Cambridge University Press (Reprinted 1993).

5. D. M. Chase 1972 *Journal of the Acoustical Society of America* **52**, 1011 - 1023. Sound radiated by turbulent flow off a rigid hal-plane as obtained from a wavevector spectrum of hydrodynamic pressure.

6. K. L. Chandiramani 1974 *Journal of the Acoustical Society of America* **55**, 19 - 29. Diffraction of evanescent waves, with applications to aerodynamically scattered sound and radiation from unbaffled plates.

7. D. M. Chase 1975 *American Institute of Aeronautics and Astronautics Journal* **13**, 1041 - 1047. Noise radiated from an edge in turbulent flow.

8. D. M. Chase 1980 *Journal of Sound and Vibration* **70**, 29 - 67. Modeling the wavevector-frequency spectrum of turbulent boundary layer wall pressure.

9. G. M. Corcos 1964 *Journal of Fluid Mechanics* **18**, 353 - 378. The structure of the turbulent pressure field in boundary layer flows.

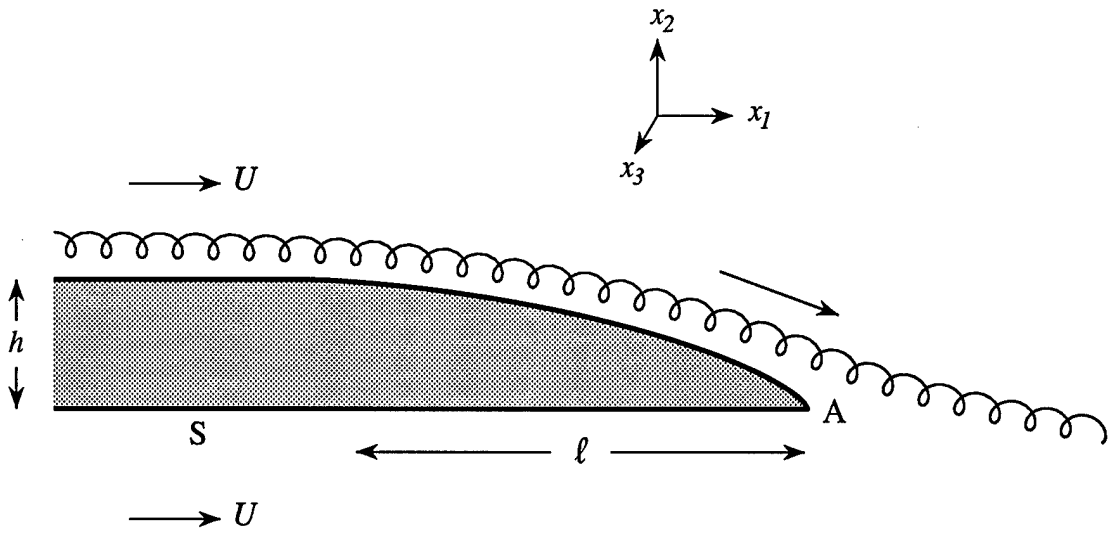

Figure 1. Schematic low Mach number turbulent boundary layer flow over a rounded trailing edge.

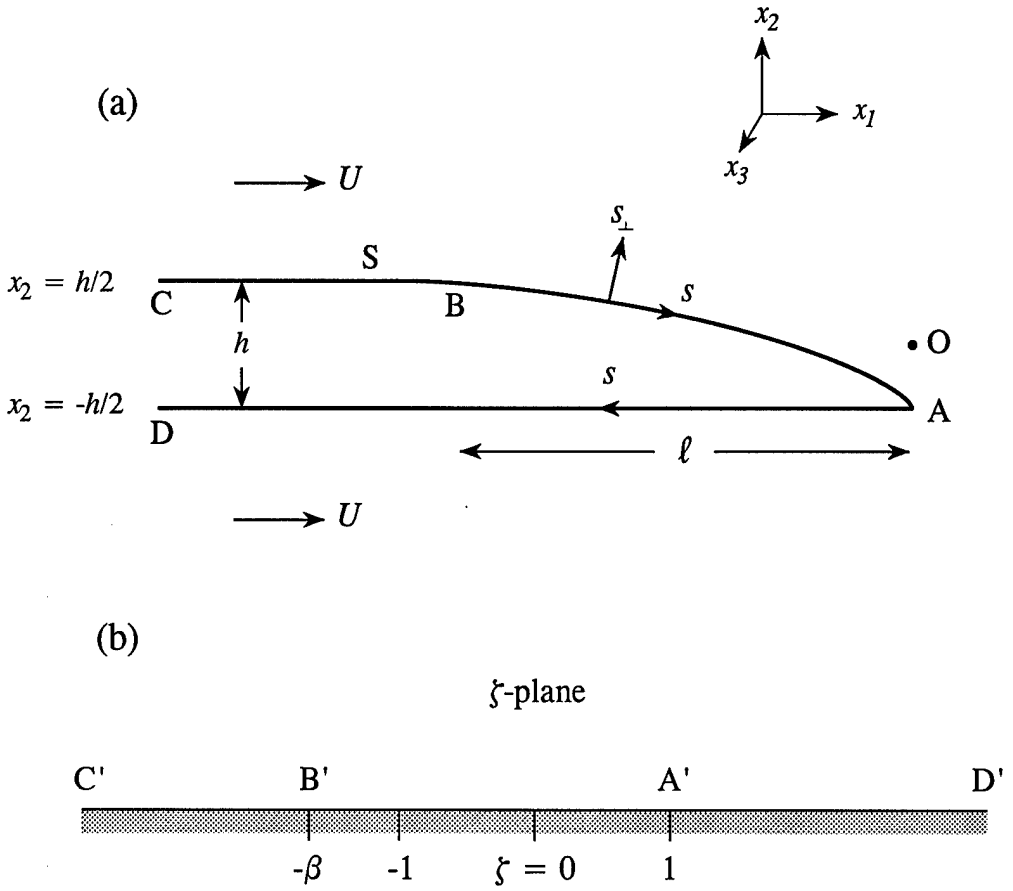

Figure 2. (a) Configuration of the trailing edge and the coordinate system. (b) Mapping the region outside the airfoil (in the plane of $z = x_1 + ix_2$) onto the upper half of the ζ-plane.

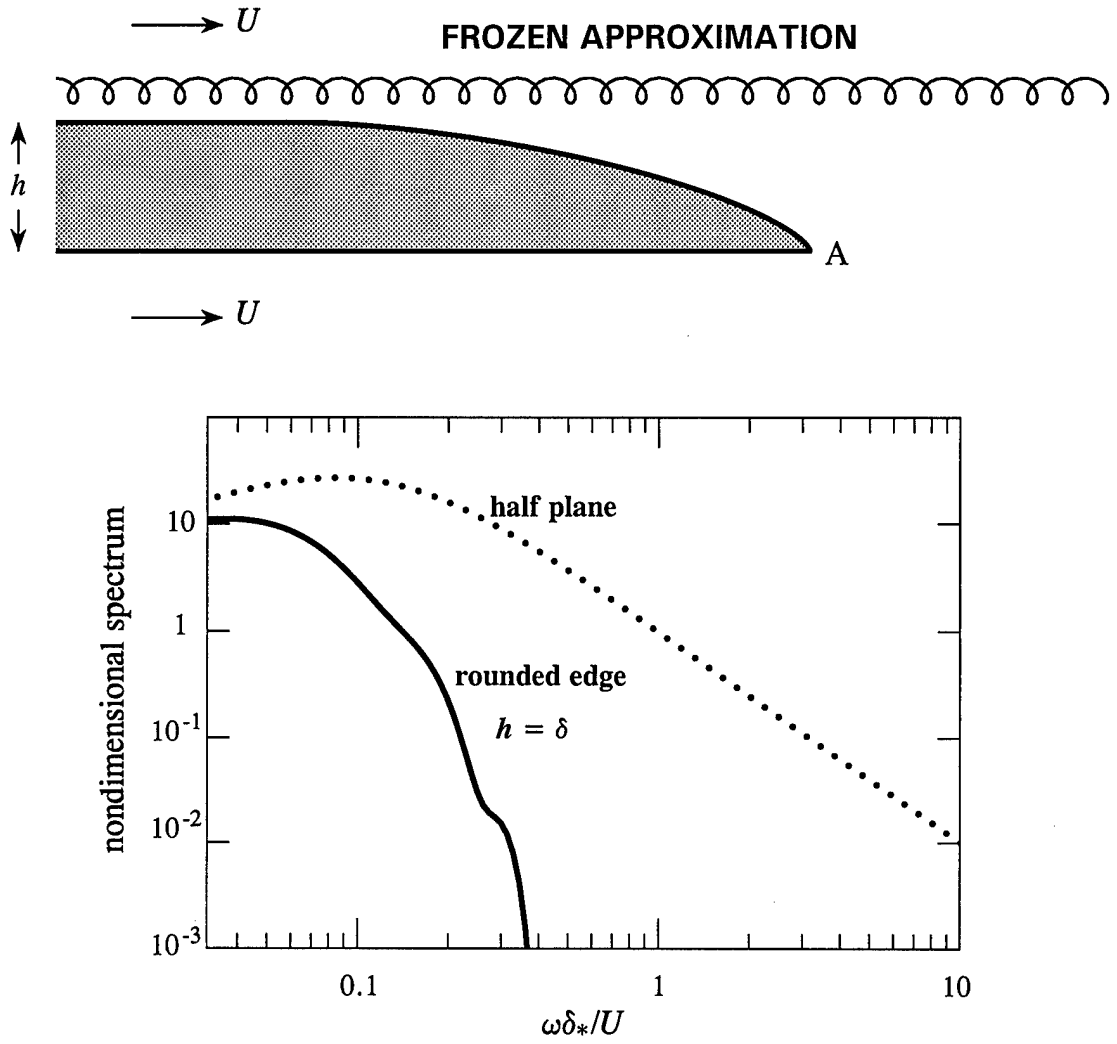

Figure 3. Frozen approximation to the edge noise spectrum $(U/\delta_*)\Phi(\mathbf{x},\omega)/[a_o(\rho_o v_*^2)^2 M(L\delta_*/|\mathbf{x}|^2)\sin\psi\sin^2(\theta/2)]$ for the rounded edge of Figure 2a of thickness $h=\delta$ when $\ell = 4h$, and for the rigid half plane ($h=0$).

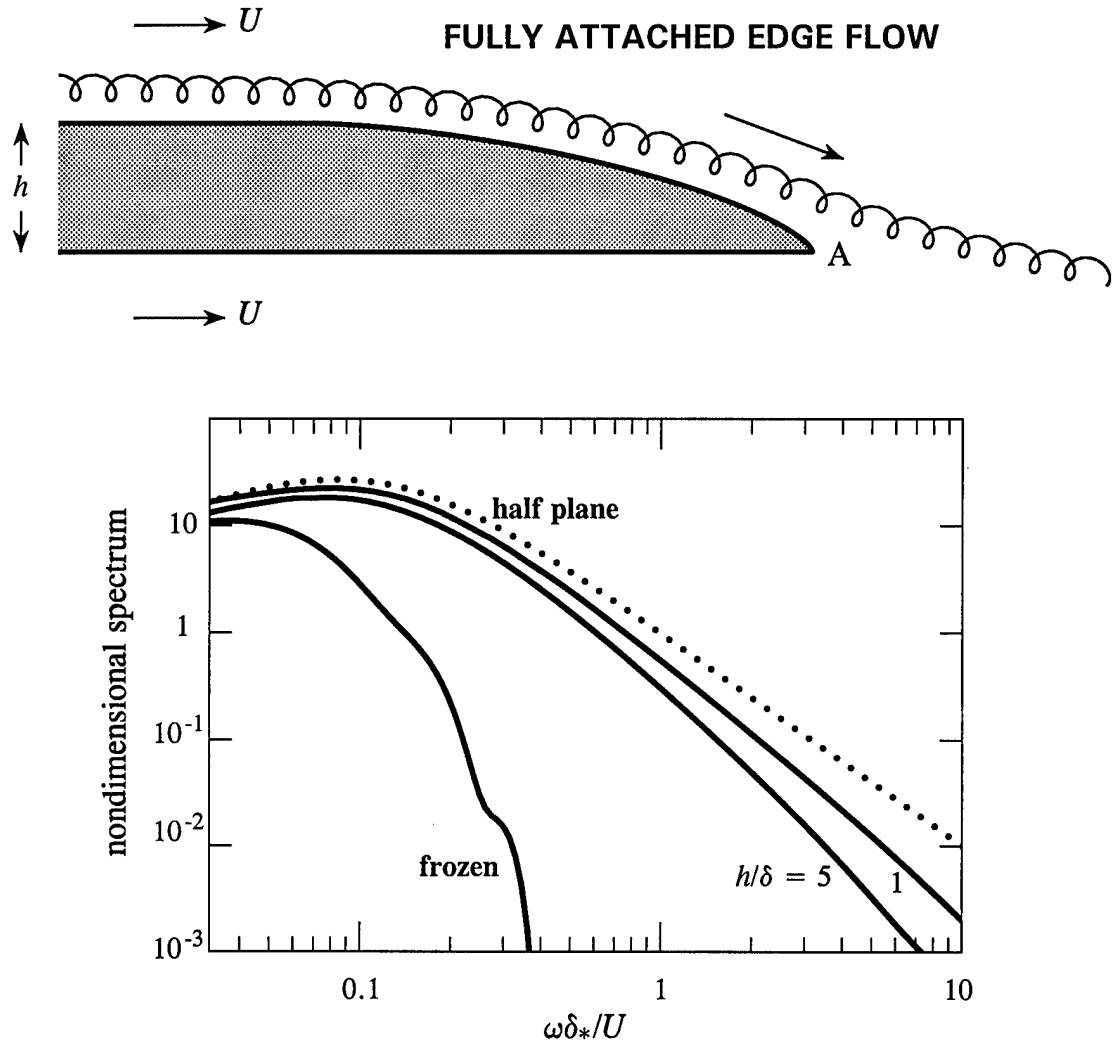

Figure 4. Predicted edge noise spectrum
$(U/\delta_*)\Phi(\mathbf{x},\omega)/[a_o(\rho_o v_*^2)^2 M(L\delta_*/|\mathbf{x}|^2)\sin\psi\sin^2(\theta/2)]$
for the rounded edge of Figure 2a of thickness $h/\delta = 1$ and 5, when $\ell = 4h$. Also shown for comparison are the frozen and half-plane spectra.

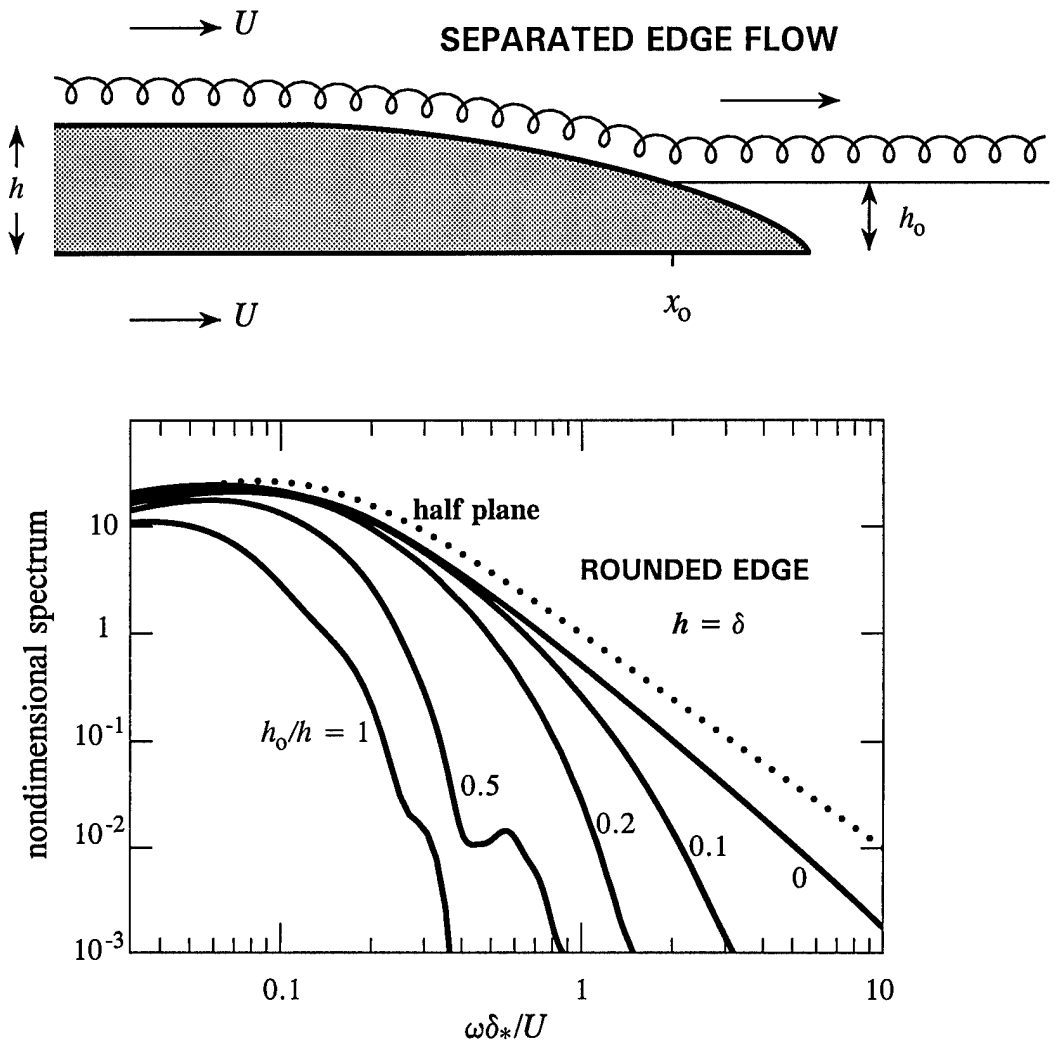

Figure 5. Predicted edge noise spectrum
$(U/\delta_*)\Phi(\mathbf{x},\omega)/[a_o(\rho_o v_*^2)^2 M(L\delta_*/|\mathbf{x}|^2)\sin\psi\sin^2(\theta/2)]$
for the rounded edge of Figure 2a when $h/\delta = 1$, $\ell = 4h$, and for the separated edge flows of Table 1.

REPORT DOCUMENTATION PAGE

Form Approved
OMB No. 0704-0188

1. AGENCY USE ONLY *(Leave blank)*	2. REPORT DATE	3. REPORT TYPE AND DATES COVERED
	9 March 1999	Final. 13 July 1998 - 28 Feb. 1999

4. TITLE AND SUBTITLE
Trailing edge noise evaluated at very low Mach number from incompressible flow simulations

5. FUNDING NUMBERS
N00014-98-1-0798

6. AUTHOR(S)
Michael S. Howe

7. PERFORMING ORGANIZATION NAME(S) AND ADDRESS(ES)
Boston University
College of Engineering
110 Cummington Street
Boston MA 02215

8. PERFORMING ORGANIZATION REPORT NUMBER
AM-99-003

9. SPONSORING/MONITORING AGENCY NAME(S) AND ADDRESS(ES)
Office of Naval Research
Code 333
Dr. L. Patrick Purtell

10. SPONSORING/MONITORING AGENCY REPORT NUMBER

11. SUPPLEMENTARY NOTES

12a. DISTRIBUTION/AVAILABILITY STATEMENT
Approved for Public Release

12b. DISTRIBUTION CODE

13. ABSTRACT *(Maximum 200 words)*

The diffraction theory of trailing edge noise is extended to determine the sound produced by very low Mach number flow over the edge of an airfoil of finite thickness. It is desired to represent the noise in terms of a surface integral over the airfoil involving a Green's function and a metric of the edge flow that can be calculated locally using equations for *incompressible* flow. The appropriate metric for a rigid airfoil is the incompressible "upwash" velocity (determined by the Biot-Savart induction formula applied to the boundary layer vorticity outside the viscous sublayer), and *not* the surface pressure. A detailed discussion is given of a two-dimensional vortex flow over an airfoil with a rounded trailing edge. An approximate method is proposed for determining the edge noise spectrum for both fully attached flow separated flow over a rounded trailing edge.

14. SUBJECT TERMS
Aerodynamic sound, edge noise, vortex sound, trailing edge, thickness effects, rounded edge

15. NUMBER OF PAGES
55 + i

16. PRICE CODE

17. SECURITY CLASSIFICATION OF REPORT	18. SECURITY CLASSIFICATION OF THIS PAGE	19. SECURITY CLASSIFICATION OF ABSTRACT	20. LIMITATION OF ABSTRACT
Unclassified	Unclassified	Unclassified	